AGU PUBLICATIONS

Geochemistry, Geophysics, Geosystems

RESEARCH ARTICLE
10.1002/2017GC007141

Special Section:
Carbon Degassing Through Volcanoes and Active Tectonic Regions

A New Sulfur and Carbon Degassing Inventory for the Southern Central American Volcanic Arc: The Importance of Accurate Time-Series Data Sets and Possible Tectonic Processes Responsible for Temporal Variations in Arc-Scale Volatile Emissions

J. M. de Moor[1,2], C. Kern[3], G. Avard[1], C. Muller[1], A. Aiuppa[4,5], A. Saballos[6], M. Ibarra[6], P. LaFemina[7], M. Protti[1], and T. P. Fischer[2]

[1]Observatorio Vulcanológico y Sismológico de Costa Rica, Universidad Nacional, Heredia, Costa Rica, [2]Department of Earth and Planetary Sciences, University of New Mexico, Albuquerque, NM, USA, [3]Cascades Volcano Observatory, U.S. Geological Survey, Vancouver, WA, USA, [4]Dipartimento DiSTeM, Università di Palermo, Palermo, Italy, [5]Istituto Nazionale di Geofisica e Vulcanologia, Sezione di Palermo, Italy, [6]Dirección de Vulcanología,Instituto Nicaragüense de Estudios Territoriales (INETER), Managua, Nicaragua, [7]Department of Geosciences, The Pennsylvania State University, University Park, PA, USA

Key Points:
- We present an extensive new data set for Central American volcanic gas emission rates
- Higher gas fluxes are observed for 2015-2016 than in previous studies, calling for expansion of gas monitoring networks
- Higher gas fluxes are related to increased arc-wide volcanic activity and may be related to megathrust earthquakes

Supporting Information:
- Supporting Information S1

Correspondence to:
J. M. de Moor,
maartenjdemoor@gmail.com

Citation:
de Moor, J. M., Kern, C., Avard, G., Muller, C., Aiuppa, A., Saballos, A., . . . Fischer, T. P. (2017). A new sulfur and carbon degassing inventory for the Southern Central American Volcanic Arc: The importance of accurate time-series data sets and possible tectonic processes responsible for temporal variations in arc-scale volatile emissions. *Geochemistry, Geophysics, Geosystems*, *18*, 4437–4468. https://doi.org/10.1002/2017GC007141

Received 17 JUL 2017
Accepted 31 OCT 2017
Accepted article online 8 NOV 2017
Published online 12 DEC 2017
Corrected 24 JAN 2018

This article was corrected on 24 JAN 2018. See the end of the full text for details.

Abstract This work presents a new database of SO_2 and CO_2 fluxes from the Southern Central American Volcanic Arc (SCAVA) for the period 2015–2016. We report ~300 SO_2 flux measurements from 10 volcanoes and gas ratios from 11 volcanoes in Costa Rica and Nicaragua representing the most extensive available assessment of this ~500 km arc segment. The SO_2 flux from SCAVA is estimated at 6,240 ± 1,150 T/d, about a factor of three higher than previous estimations (1972–2013). We attribute this increase in part to our more complete assessment of the arc. Another consideration in interpreting the difference is the context of increased volcanic activity, as there were more eruptions in 2015–2016 than in any period since ~1980. A potential explanation for increased degassing and volcanic activity is a change in crustal stress regime (from compression to extension, opening volcanic conduits) following two large (Mw > 7) earthquakes in the region in 2012. The CO_2 flux from the arc is estimated at 22,500 ± 4,900 T/d, which is equal to or greater than estimates of C input into the SCAVA subduction zone. Time-series data sets for arc degassing need to be improved in temporal and spatial coverage to robustly constrain volatile budgets and tectonic controls. Arc volatile budgets are strongly influenced by short-lived degassing events and arc systems likely display significant short-term variations in volatile output, calling for expansion of nascent geochemical monitoring networks to achieve spatial and temporal coverage similar to traditional geophysical networks.

Plain Language Summary We show that volcanoes in Central America are more active now than any time in the scientific record, and explore possible causes.

1. Introduction

Convergent margins are the Earth's interface between shallow and deep geochemical reservoirs. Here, subduction of oceanic crust provides the primary mechanism by which volatile elements may be recycled back to the mantle (e.g., Dasgupta, 2013). Release of volatiles from the subducted slab is also the driving force behind arc volcanism, which tends to be more gas-rich, explosive, and hazardous than intraplate or rift volcanism. Quantifying volcanic degassing from active arcs is a fundamental constraint needed for assessing the proportion of subducted volatiles that is returned to the surface versus that retained in the slab beyond the volcanic front and carried to the deep mantle (e.g., Evans, 2012).

Accurate measurement of gas emission rates from volcanoes is challenging on many levels. Sulfur dioxide is the primary gas species typically used for estimating volcanic gas flux due to its high concentration in magmatic gases, very low background concentration in ambient air, and because it can be measured using ground-based remote methods as it strongly absorbs UV light, making it feasible to routinely measure SO_2

emission rates (e.g., Stoiber et al., 1983). Today, traverse measurements with vertically pointing mobile-DOAS (Differential Optical Absorption Spectroscopy; Galle et al., 2002) are probably the most widely used and accepted method for determining accurate SO_2 fluxes from degassing volcanoes. Satellite measurements typically have high detection limits, and are thus only applicable to volcanoes in eruptive phases or during periods of relatively strong passive degassing (e.g., Carn et al., 2013). For a given volcano, compilations of SO_2 fluxes estimated from satellite measurements probably overestimate time-integrated SO_2 fluxes as periods where no degassing is detected are not considered in deriving a mean, perhaps artificially skewing estimates to higher values by taking the mean of detected volcanic plumes only. The accuracy of satellite gas flux measurements is also dependent on wind-speed estimates derived from global weather models. Permanent scanning DOAS stations to monitor SO_2 flux provide relatively high temporal resolution and robust long-term monitoring stations (Galle et al., 2010) but these measurements are in many cases imprecise due to high uncertainties in plume position, environmental conditions, and plume speed. New technologies such as UV cameras promise to revolutionize SO_2 flux monitoring by providing very high temporal resolution emission rates with internally consistent plume-speed measurements (Kern et al., 2015) as well as spatial resolution (D'Aleo et al., 2016), but also have high detection limits relative to the more sensitive DOAS. Accurate SO_2 fluxes with UV cameras also are more challenging due to radiative transfer problems such as light dilution and the limited spectral information collected (Campion et al., 2015; Kern et al., 2010).

The strong absorption of UV light by SO_2 and its very low atmospheric background allow SO_2 fluxes to be measured remotely and with relative ease compared to direct flux measurements of other volcanic gas species. The emission rates of other gases are often calculated from the product of the SO_2 flux with the ratio of the species of interest to SO_2, obtained from gas composition analysis (e.g., direct sampling, Multi-GAS, open-path FTIR). Global estimates of arc degassing have typically depended on a relatively small number of high-temperature gas samples to approximate a gas composition taken as representative for a given arc segment (Fischer, 2008; Hilton et al., 2002). These studies attain estimates of arc degassing fluxes for all major volcanic volatiles (H_2O, CO_2, HCl, HF, He, etc.) usually based on the compilation of SO_2 fluxes from Andres and Kasgnoc (1998), which were measured between 1979 and 1998, and extrapolations based on power law distribution of volcanic degassing (Brantley & Koepenick, 1995) to estimate the total arc gas flux. However, in the most extensive detailed assessment of SO_2 fluxes from an arc segment to date, Mori et al. (2013) show that volcanoes along the Japanese arc do not follow a power law distribution and the total SO_2 flux was significantly higher (by about 50%) than previous estimates. More recent compilations of CO_2 flux (e.g., Burton et al., 2013) have used various surveys conducted since the 1950s via a variety of methods to estimate the global CO_2 flux, and large extrapolations (e.g., Perez et al., 2011) to estimate total global gas fluxes. Recently, Carn et al. (2017) provided an updated global inventory of SO_2 fluxes based on a 10 year (2005–2015) satellite database, resulting in an estimated SO_2 flux of 23.0 ± 2.3 Tg/yr (63.0 ± 6.3 kT/d) and also identified arc-scale temporal variations in SO_2 degassing for the first time. Their global SO_2 flux estimate is about double that estimated by Andres and Kasgnoc (1998) from ground-based measurements. Although Carn et al. (2017) acknowledge that limitations in spatial resolution and wind-speed estimates may introduce large systematic uncertainties into the accuracy of satellite-based SO_2 fluxes (especially for high and low gas emitters), these errors will not affect interannual flux variability.

Volcanic gas emissions from Southern Central American Volcanic Arc (SCAVA; from southern Costa Rica to northern Nicaragua; ~500 km) have been intensely studied in comparison to many other arc segments, and volatile fluxes from this region would be considered well-characterized in global data sets. However, most previous studies have in fact focused on gas compositions or studies of fluxes at only a few volcanoes. Calculations of volatile mass balance at the arc (Elkins et al., 2006; Fischer, 2008; Fischer et al., 2002; Hilton et al., 2002; Shaw et al., 2003; Zimmer et al., 2004) have mostly been based on early measurements of gas fluxes by Andres and Kasgnoc (1998) with a number of updates (Aiuppa et al., 2014; Mather et al., 2006), though these studies typically rely on previous studies for a significant proportion of the total reported flux.

Here, we provide new (2015–2016) ground-based campaign DOAS measurements to constrain SO_2 flux at volcanoes along a ~500 km section of the Central America Volcanic Arc in Costa Rica and Nicaragua (Figure 1). Combined with compositional data from Multi-GAS measurements, we estimate emission rates for SO_2 and CO_2 from all of the ten actively degassing volcanoes from this arc segment.

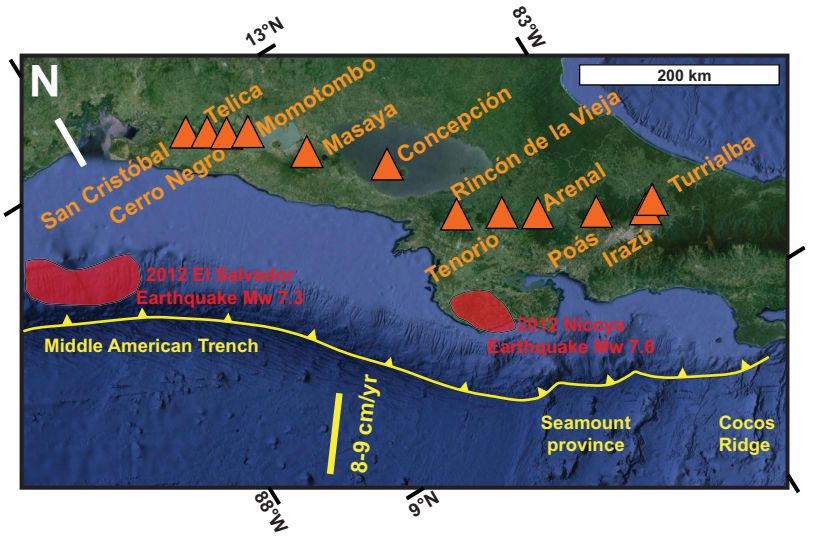

Figure 1. Map of Southern Central American Arc showing major active volcanic centers, all of which were investigated in this work, and the areas of slip during the 2012 El Salvador and Nicoya earthquakes.

2. Methods

The primary methods used in this study are vertical-pointing, differential optical absorption spectroscopy (DOAS) to estimate SO_2 emission rate and multiple gas analyzer systems (Multi-GAS) to constrain CO_2/SO_2. The emission rate of CO_2 is quantified by the product of the SO_2 emission rate and the CO_2/SO_2 mass ratio.

2.1. DOAS Traverses and SO_2 Retrievals

The SO_2 emission rates were measured by transporting the vertically pointing DOAS instruments below the plume either by vehicle or on foot, depending on the conditions and access (Figure 2). Sulfur dioxide column densities were retrieved from acquired spectra using a conventional DOAS retrieval (e.g., Platt & Stutz, 2008). First, a dark spectrum collected before each traverse was subtracted from all measurement spectra to correct for detector dark current and electronic offset. Any potential contribution from stray light in the spectrometer was then corrected by subtracting the average intensity measured at wavelengths shorter than 290 nm, where the ozone layer blocks incident solar radiation, from all measurement spectra. Next, the measurement spectra were converted to optical depth by dividing each one by a plume-free spectrum and taking the logarithm.

To derive the SO_2 column density above the DOAS instrument, the following references were fit to each optical depth spectrum: (1) the absorption cross sections of SO_2 and O_3(Bogumil et al., 2003; Vandaele et al., 2009), each convolved by the instrument line shape to account for the limited instrument resolution, (2) a Ring correction spectrum accounting for the variable contribution of inelastic scattering to the measurement spectra (Grainger & Ring, 1962), and (3) first-order linear corrections accounting for potential slight variations in wavelength calibration of the spectrometer (Beirle et al., 2013), as well as a third-order polynomial to account for broadband variations in the spectrum during individual traverses. The spectral fit was performed between 310 and 330 nm. However, whenever high SO_2 columns were encountered, the lower bound of the fit window was dynamically adjusted (hereafter referred to as the sliding fit window method) toward longer wavelengths such that SO_2 optical depths larger than 0.1 were avoided, as strongly absorbing gases can complicate atmospheric radiative transfer and the DOAS retrieval process (Kern et al., 2010; Platt & Stutz, 2008).

The calculation of emission rate involves integration of the SO_2 column densities obtained along the traverse perpendicular to the plume travel direction (Figure 2). In order to obtain a quantitative measure of plume direction and the associated error, we fit a Gaussian curve to the time series of SO_2 column densities measured during each traverse. The plume direction was derived by determining the vector from the emission point to the center of the Gaussian. The width of the Gaussian yields the uncertainty of the plume

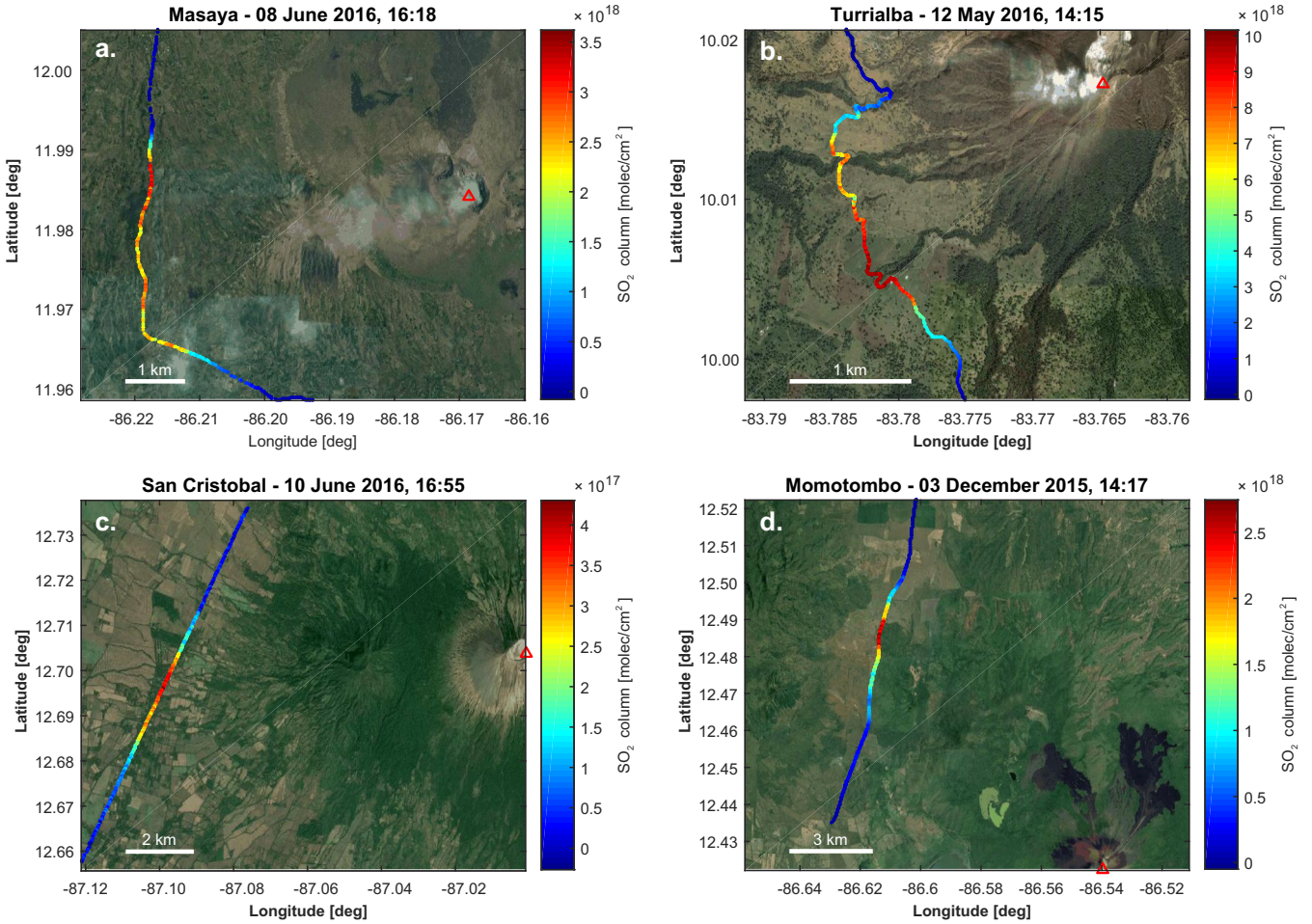

Figure 2. Examples of DOAS driving traverse conducted at (a) Masaya, (b) Turrialba, (c) San Cristobal, and (d) Momotombo volcanoes. Red triangles show plume source location and color of individual points along traverses correspond to SO_2 column amount in molecules/cm^2, with color scales shown to the right of each map.

direction. The integrated cross-sectional SO_2 burden (molecules.m^2) was multiplied by the wind speed (m/s) to obtain the SO_2 emission rate. An error estimate was made for each derived emission rate based on propagation of errors associated with the plume direction, plume speed, and the spectroscopic errors associated with the SO_2 column density retrievals.

2.2. Plume Speed

The largest source of error in calculating SO_2 emission rate by DOAS is due to wind speed estimates (e.g., Williams-Jones et al., 2006). Here we use "calibrated" wind speeds obtained from the NOAA National Center for Environmental Predictions (NCEP) Global Forecast System at 1° resolution (e.g., Conde et al., 2013; Hilton et al., 2007) as these are the only data available for all traverse measurements, thus providing internal consistency within the data set. We calibrate the NOAA model estimates based on anemometer measurements conducted at the summits of a number of volcanoes, as well as with measurements of plume speed by dual stationary vertically-pointing DOAS (Williams-Jones et al., 2006) in order to realistically assess the errors involved in plume speed estimations.

The NOAA model reports wind speeds for discrete elevations (every 500 m.a.s.l.) every 3 h. The height of the plume was estimated visually, typically being a few hundred meters above the elevation of the crater due to thermal buoyancy. The wind speed used from the NOAA model thus has an internal uncertainty derived from the fact that plume heights are not well constrained and that the measurement times do not correspond to the exact times for which NOAA values are reported. Therefore, the average of the NOAA values bounding the measurement time and plume height (consisting of between 4 and 6 individual wind

Table 1
Comparison of Plume Speed Estimates at Some SCAVA Volcanoes

Date	Volcano	NOAA (m/s)	±	Anemometer (m/s)	±	Dual vertical DOAS (m/s)	±
18/1/2014	Turrialba	9.4	1.3			9.9	1.2
15/3/2014	Turrialba	4.8	1.2	4.2	1.3	6.7	1.2
22/5/2014	Turrialba	3.7	0.6			6.1	1.2
04/9/2014	Turrialba	4.5	1.1	4.4	0.5		
28/1/2015	Turrialba	13.6	0.4	10.8	0.3		
23/1/2014	Poás	8.1	1.0	5.2	0.5	4.6	0.4
30/9/2014	Poás	4.1	0.7	6.4			
20/7/2016a	Masaya	8.4	1.6			9.1	1.2
20/7/2016b	Masaya	6.3	0.9	5.7	2.8		
21/7/2016	Masaya	8.0	0.6	6.9	4.2		
21/2/2016	Masaya	13.6	0.7	13.0	3.5		
15/11/2015	Masaya	6.7	1.2	4.5	2.1		
12/7/2016	Concepción	10.8	1.0	9.6	2.9		
17/7/2016	San Cristobal	9.2	1.0	8.7	2.8		

speed values) is used. This approach further allows us to estimate the internal precision of these values, which is about ± 0.9 m/s (average standard deviation). This represents an internal uncertainty of about 14% in the adopted wind speed values derived from the NOAA model, though it is significantly higher at low wind speeds.

Though the internal variability of the NOAA wind speed gives some measure of precision, the accuracy of gas emission rates is of utmost importance in assessing volatile budgets and mass balance at subduction zones. In order to provide a more realistic evaluation of the uncertainty in our SO_2 emission rates, we have compared the NOAA model results with direct measurement methods of plume speed determination for a subset of our measurements for which multiple plume speed determinations were conducted. The direct measurement methods of plume speed determination include: (1) hand-held anemometer readings conducted at the summits of Masaya, San Cristobal, Concepción, Poás; (2) Permanent weather station data for Turrialba volcano, which is the only volcano measured here by DOAS with a permanent weather station on its summit, and (3) dual vertically-pointing DOAS following the method of Williams-Jones et al. (2006), which we conducted at Poás (de Moor et al., 2016b), as well as at Turrialba and Masaya volcanoes, the two most significant degassing volcanoes on the arc.

The results of the wind speed comparisons are show in Table 1 and Figure 3. A good correlation ($R^2 = 0.82$) exists between the NOAA model data and the anemometer data (grouping together the handheld anemometer and permanent station data in Figure 3). The spread in the data is larger at lower wind speeds. Based on the correlation between NOAA model data and anemometer data, the NOAA model typically returns higher wind speeds than directly measured wind speeds by a factor of 1.119, which is similar to the "bias" reported by Conde et al. (2013). As simultaneous direct measurements of wind speed are only available for a small number of our traverse measurements, we use NOAA model wind speeds divided by 1.119 for all of our SO_2 traverses, thus maintaining internal consistency within the data set. In order to describe the uncertainties in the wind speed, which is essential in realistically characterizing the errors in our SO_2 flux measurements, we adopt an ad hoc approach based on the relationship between NOAA model and directly measured wind speed by defining an error envelope that encompasses the majority of the data shown in Figure 3. This approach allows us to assign larger error at lower wind speeds. Figure 3 shows the error as a function of wind speed as derived from the comparison between directly measured and NOAA model wind speed data.

All SO_2 traverse data were first assessed using 1 m/s wind speed and SO_2 flux @ 1 m/s is reported in supporting information Table S1. The NOAA model was used to determine wind speed at the volcano location for altitudes and times spanning the plume height and measurement time. The NOAA wind speed value was then divided by a value of 1.119 to provide a correction based on direct wind speed measurements. Errors were assigned to these corrected values as a function of the corrected wind speed value. Summarized daily SO_2 fluxes and errors are reported in Table 2. We note that dual vertically pointing DOAS is considered

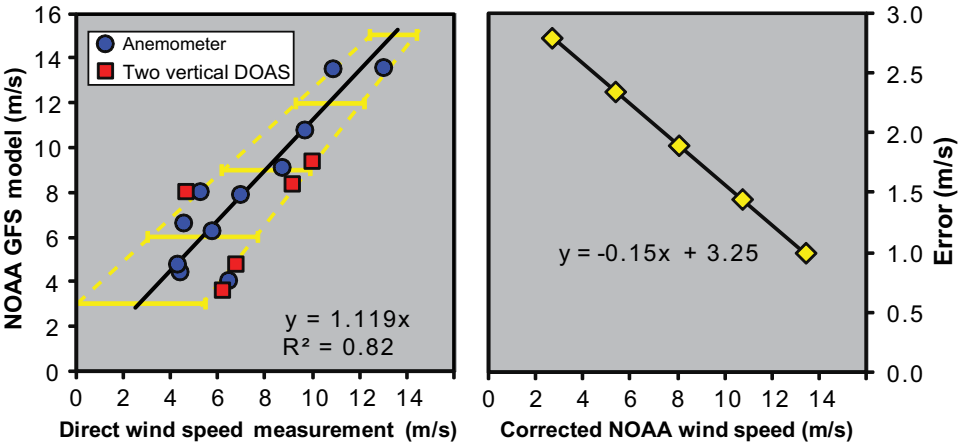

Figure 3. Comparison of NOAA GFS model results with direct wind speed measurements by anemometer (blue circles) and dual vertical DOAS measurements (red squares). Based on the observed correlation in left plot, the NOAA are corrected and used in calculating SO_2 fluxes. Error estimates in the corrected wind speed values are derived from the error envelope shown in the left plot (yellow bars and dashed yellow lines). The right plot shows relationship between corrected NOAA wind speed and error assumed based on the spread of data in left plot. The uncertainty in wind speed (and calculated SO_2 flux) increases with decreasing wind speed.

the most accurate determination of true plume travel speed and gives higher plume speeds than the other methods. The one exception to this was observed at Poás, where local topography plays a strong role in decreasing the wind speed at the measurement site. Our correction based on both the dual-beam DOAS and the anemometer measurements thus yields conservative values for wind speed and SO_2 emission rate.

2.3. Multi-GAS Methods

Multi-GAS data were collected via fixed automated stations at Turrialba and Masaya volcanoes, and by campaign measurements at Irazú, Poás, Arenal, Tenorio, Miravalles, Rincón de la Vieja, Cerro Negro, Telica, and San Cristobal volcanoes. Campaign measurements were also conducted at Masaya when technical problems with the automated station resulted in data gaps in the high-frequency time series. Details of these specific Multi-GAS instruments used in this study are given in de Moor et al. (2016a, 2016b).

The fixed instruments record gas concentrations of SO_2, H_2S, CO_2, and H_2O at a rate of 0.1 Hz for 30 min four times a day with data telemetered in near-real time. The mobile Multi-GAS unit records data every 2 s, with data acquisition started and stopped manually by the operator. Gas ratios (CO_2/SO_2, H_2S/SO_2, H_2O/SO_2) are derived from linear regression through the concentration data and are independent of mixing with air (Aiuppa, et al., 2007, 2009, 2014; de Moor et al., 2016a, 2016b). Total errors in gas ratios as measured by Multi-GAS are $<$20% (de Moor, et al., 2016b). Figure 4 shows examples of Multi-GAS data acquired at magmatic and hydrothermal systems at SCAVA.

3. Results

Full DOAS traverse results are presented in supporting information Table S1 and summarized in Table 2 as daily average SO_2 fluxes (see sections 4.1.1 and 4.1.2). The data presented in Table 2 represent our best estimates of persistent passive degassing from the active volcanoes in SCAVA. The data were filtered (see supporting information for details) to remove traverses conducted under unacceptably poor weather conditions or during transient eruptive or nonrepresentative events. The filtering process reduced the total number of traverses considered from 308 to 260.

Turrialba and Masaya dominate the total SO_2 flux from the arc, together accounting for 83% of the total. Turrialba has emitted an average of 2,990 $\pm$ 980 T/d in 2015–2016 and has been the largest volatile emitter at SCAVA since a significant escalation in degassing intensity following the 29 October 2014 eruption (de Moor et al., 2016a). The total SO_2 flux decreased significantly at Poás between 2014 (de Moor et al., 2016b) and 2016, followed by a dramatic increase during the 2017 phreatomagmatic eruption (unpublished data). Full results of changes in gas compositions and fluxes for Poás will be presented in a separate contribution.

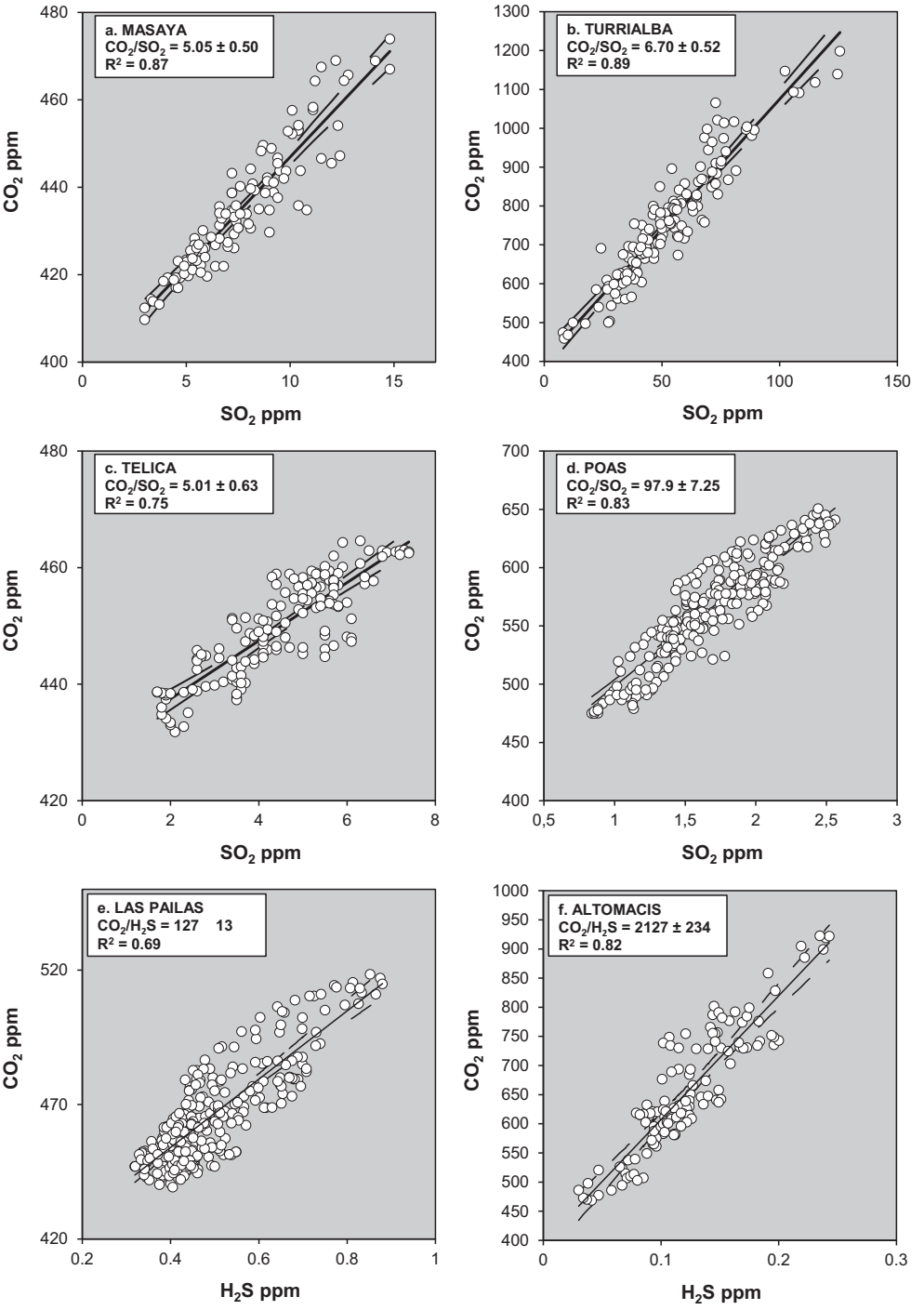

Figure 4. (a–d) Examples of CO_2 versus SO_2 plots from Multi-GAS data collected at (a) Masaya, (b) Turrialba, (c) Telica, and (d) Poás volcanoes, respectively. The CO_2/SO_2 ratio is the slope of the linear regression. Plots (e) and (f) show CO_2 versus H_2S at hydrothermal systems Las Pailas (flanks of Rincón de la Vieja volcano) and Altomacis (flanks of Tenorio volcano) where no SO_2 is present.

No SO_2 has been detected at Arenal volcano since 2014. Rincón de la Vieja data in Table 2 are taken from de Moor et al. (2016b). Concepción is a low but persistently degassing volcano, with an average SO_2 flux of ~40 T/d. Masaya is the most persistently degassing volcano on the arc and our measurements yield an average of 1,880 ± 510 T/d for 2015–2016. We have conducted more than 100 traverse measurements at Momotombo volcano since the 2 December 2015 eruption, observing very high fluxes up to >3,000 T/d in

Table 2
Summary of SO_2 Flux Data Set for 2015–2016 Listed by Volcano From South to North

Volcano	Date	SO_2 flux T/d	Error T/d	N
Turrialba	29/12/2014	2,810	630	4
	22/4/2015	3,910	1,060	4
	18/12/2015	2,400	1,380	4
	06/4/2016	1,780	270	4
	12/5/2016	4,890	2,100	3
	17/5/2016	3,770	1,000	2
	08/9/2016	1,340	500	2
Poás	26/5/2015	109	25.0	2
	27/8/2015	67.0	29.4	2
	01/10/2015	36.3	10.3	3
	01/2/2016	24.9	10.5	2
	07/4/2016	26.8	10.5	7
	07/6/2016	16.8	7.30	6
	05/8/2016	46.5	16.1	4
Arenal	17/4/2014	0	1	3
	27/5/2015	0	10	3
Rincón de la Vieja	14/4/2014	66.0	17.0	10
Concepcion	10/6/2015	27.9	22.9	5
	13/7/2016	50.7	63.4	3
Masaya	15/11/2015	1,660	440	5
	26/2/2016	877	170	11
	10/3/2016	2,990	500	9
	28/4/2016	1,040	520	5
	22/6/2016	3,780	1,520	5
	29/6/2016	3,180	530	8
	07/7/2016	4,020	610	2
	12/7/2016	5,020	700	6
	15/7/2016	1,570	330	7
	17/7/2016	4,330	590	4
	20/7/2016	1,730	470	12
	21/7/2016	2,500	540	10
Momotombo	02/2/2016	530	278	6
	07/2/2016	655	240	2
	10/2/2016	1,160	220	9
	22/2/2016	387	125	15
	24/2/2016	684	344	5
	25/2/2016	957	165	13
	03/3/2016	697	246	9
	16/6/2016	374	227	6
	16/7/2016	201	63.0	6
Cerro Negro	20/11/2015	0	2	2
Telica	24/6/2016	244	176	1
	16/7/2016	361	172	3
	17/7/2016	201	118	2
San Cristobal	10/6/2016	407	208	7
	24/6/2016	365	163	5
	14/7/2016	445	180	4
	16/7/2016	274	108	8
	17/7/2016	178	93.0	2
TOTAL ARC FLUX	2015–2016	6,150	1,150	262

Note. Daily average SO_2 fluxes were calculated using a sliding fit window and are reported with error and number of traverses considered. Full data are reported in supporting information (Table S1).

late 2015 and early 2016 associated with short-lived explosive events (supporting information Table S1) and have recorded a decrease in gas flux down to background levels by mid-2016. Only background SO_2 fluxes (i.e., not associated with short-lived explosions) are reported in Table 2. No SO_2 was detected by DOAS at Cerro Negro. Telica and San Cristobal both emit moderate amounts of SO_2 at ~300 T/d.

Multi-GAS results are reported in Tables 3 and 4. Data are reported from both mobile (campaign measurements) and permanent (fixed instruments; four measurements per day) Multi-GAS stations. Table 3 reports gas ratios from volcanoes where SO_2 is a component of the emissions, here considered "magmatic" gas

Table 3
Multi-GAS Data for SCAVA Volcanoes With Magmatic Gas Compositions Listed by Volcano From South to North

Magmatic gases	Multi-GAS type	Max SO_2 ppm	CO_2/SO_2	±	H_2S/SO_2	±	H_2O/SO_2	±
Turrialba								
29/12/2014	Permanent	36.6	6.3	2.1	1.11	0.22	17	5
19–20/4/2015	Permanent	90.6	1.5	0.5	<dl	<dl	na	na
18–19/12/2015	Permanent	24.9	23.3	7.3	2.28	0.27	16	3
6/4/2016	Permanent	78.4	2.0	0.4	<dl	<dl	12	3
12/5/2016	Permanent	107.9	4.8	1.2	0.03	0.03	3	1
17/5/2016	Permanent	165.4	3.2	0.5	<dl	<dl	8	2
8/9/2016	Permanent	2.7	2.7	0.2	0.07	0.01	na	na
25–26/9/2016	Permanent	11.0	2.5	0.1	0.08	0.00	na	na
Poás Fumaroles								
9/2/2015	Mobile	127.2	0.4	0.3	0.45	0.08	6	2
17/6/2015	Mobile	33.9	1.0	0.1	0.66	0.02	na	0
27/8/2015	Mobile	13.4	2.0	0.4	na	Na	63	9
1/10/2015	Mobile	76.8	1.5	0.1	0.67	0.01	120	8
1/2/2016	Mobile	67.3	1.1	0.1	0.67	0.01	92	7
7/4/2016	Mobile	14.9	2.8	na	0.78	Na	344	na
4–8/4/2016	Permanent	8.1	2.9	na	0.74	0.00	na	na
7/6/2016	Mobile	22.4	4.7	0.7	0.10	0.02	424	580
10/6/2016	Permanent	5.3	5.2	na	0.03	0.00	0	0
5/8/2016	Mobile	2.8	114.2	11.3	0.67	0.05	1331	139
Poás Lake								
2/1/2015	Mobile	1.5	1.5	0.9	<dl		na	na
17/6/2015	Mobile	8.7	8.7	1.1	<dl		105	14
27/8/2015	Mobile	4.4	4.4	0.5	<dl		46	6
1/10/2015	Mobile	6.1	6.1	0.4	<dl		235	24
1/2/2016	Mobile	9.3	9.3	0.8	<dl		192	20
7/4/2016	Mobile	4.1	4.1	0.0	<dl		161	na
7/6/2016	Mobile	4.3	4.3	0.3	<dl		296	336
4/8/2016	Permanent	4.5	4.5	0.8	<dl		na	na
Rincón de la Vieja								
8/4/2013	Mobile	1.2	27.0	16.3	0.94	0.20	5423	?
14/4/2014	Mobile	8.1	6.9	3.9	0.36	0.16	na	na
3/10/2014	Mobile	17.0	4.3	1.5	0.05	1.53	144	?
8/3/2016	Mobile	4.7	9.5	5.0	<dl		293	?
Masaya								
16/11/2015	Permanent	14.9	6.9	0.8	<dl	<dl	20	na
25/2/2016	Permanent	5.9	9.7	1.3	<dl	<dl	23	na
26/2/2016	Permanent	10.2	10.1	1.2	<dl	<dl	12	3
29/2/2016	Permanent	12.8	6.6	0.7	<dl	<dl	14	4
1/3/2016	Permanent	5.7	7.7	1.2	<dl	<dl	26	6
22/4/2016	Mobile	20.5	6.3	0.7	<dl	<dl	82	9
28/4/2016	Mobile	28.9	7.3	0.4	<dl	<dl	62	3
14/7/2016	Mobile	31.1	3.7	0.2	<dl	<dl	47	6
15/7/2016	Mobile	29.6	3.8	0.2	<dl	<dl	47	5
20/7/2016	Permanent	5.3	3.1	0.7	<dl	<dl	na	
21/7/2016	Mobile	23.8	4.8	0.2	<dl	<dl	69	5
21/7/2016	Permanent	12.4	4.7	1.0	<dl	<dl	98	na
Cerro Negro								
21/11/2015	Mobile	3.0	147.5	9.2	0.33	0.03	2911	321
Telica								
27/4/2016	Mobile	7.4	6.1	1.1	<dl	<dl	194	24
San Cristobal								
17/7/2016	Mobile	15.2	4.8	0.7	<dl	<dl	85	8

Note. See full results in Table S2.

Table 4
Multi-GAS Data for SCAVA Volcanoes With Hydrothermal Gas Compositions Listed by Volcano From South to North

Hydrothermal gases	Max H_2S ppm	CO_2/H_2S	±	H_2/CO_2	±	H_2O/CO_2	±
Irazú-North Flank							
11/11/2013	29	31.0	2.1	na	na	Na	na
23/5/2014	39	34.2	3.5	0.020	0.005	1.6	0.2
30/12/2014	70	43.9	2.1	0.0002	na	0.1	0.0
4/1/2016	30	41.8	6.2	na	na	Na	na
Arenal–Crater							
21/4/2014	9.3	418	52	0.0037	0.0009	54.6	8.5
Tenorio–Altomasis							
2/11/2016	0.7	1,530	280	0.0010	0.0003	0.4	0.1
Rincón de la Vieja-Las Pailas							
4/10/2014	1.3	150	20	0.0010	0.0003	146.5	24.0

Note. Full results in Table S3.

compositions whereas gases that completely lack SO_2 and contain H_2S as the only detectable S species are considered "hydrothermal" (Table 4). The maximum SO_2 or H_2S concentration recorded is used as an indicator of plume intensity and signal strength. Gas ratios are reported with SO_2 as the denominator in the case of magmatic systems and ratios are reported relative to CO_2 for the hydrothermal systems.

Gas ratios have varied dramatically at Turrialba since 2014, with CO_2/SO_2 in our data set ranging from 1.5 ± 0.5 to 23.3 ± 7.3. Irazú volcano shows H_2S-rich hydrothermal gas compositions with CO_2/H_2S from 31 ± 2.1 to 43.9 ± 2.1. Very large temporal variations in gas compositions have also been recorded at Poás volcano, with fumarolic CO_2/SO_2 ranging from 0.4 ± 0.3 to 114 ± 11. More subdued compositional variations have been observed in the Poás acid lake emissions, with CO_2/SO_2 from 1.5 ± 0.9 to 9.3 ± 0.8. Arenal gas compositions are hydrothermal in character and do not contain SO_2, even though fumarole temperatures were ~400°C in 2014. Rincón de la Vieja gas compositions show significant variations, with CO_2/SO_2 ranging from 4.3 ± 1.5 to 27 ± 16. Masaya volcano has shown high CO_2/SO_2 up to 10.1 ± 1.2 that preceded the appearance of a lava lake. The CO_2/SO_2 decreased significantly in 2016 to values down to 3.1 ± 0.7. Cerro Negro degassing is currently characterized by low-flux moderate-temperature fumaroles that emit relatively S-poor gas. CO_2/SO_2 was 147 ± 9 at the time of our measurements, with H_2S/SO_2 0.30 ± 0.03. Telica measurements show CO_2/SO_2 of 6.1 ± 1.1 whereas San Cristobal measurements yielded 4.8 ± 0.7. No H_2S was detected at Masaya, Telica, San Cristobal, or from Poás crater lake. Turrialba has shown a dramatic decrease in H_2S to below detection limit since the beginning of 2016. Poás fumaroles and Cerro Negro show significant H_2S. Hydrothermal gas compositions show large variations in CO_2/H_2S, from >1,000 at Altomasis site (Tenorio volcano flank) to more H_2S-rich compositions at Irazú ($CO_2/H_2S \sim 40$). Hydrothermal gases contain detectable H_2, with the most H_2-rich gases observed at Las Pailas (Rincón de la Vieja flank).

4. Discussion

4.1. Gas Fluxes, Selection of Representative Measurements, and Eruptive Activity

Andres and Kasgnoc (1998), Fischer (2008), and Burton et al. (2013) highlighted that passively degassing volcanoes account for the vast majority of the global volcanic S emissions. Following Andres and Kasgnoc (1998), Hilton et al. (2002) only considered SO_2 flux data from passively degassing volcanoes in deriving their inventory of global arc gas emissions. Similarly, Shaw et al. (2003) adopted the same approach in assessing the carbon budget for the Central American arc.

Many of the volcanoes measured in this study displayed some sort of unrest during the period of investigation. These manifestations include frequent low energy and relatively dilute ash emissions from Turrialba, the first magmatic eruption at Momotombo in 150 years, a moderate vulcanian eruption at Telica that produced an 8 km ash column, numerous phreatic eruptions at Poás and Rincón de la Vieja volcanoes, the appearance of a lava lake at Masaya, and anomalous seismic swarms at Concepción. Figure 5 shows time-series plots of SO_2 flux data for selected volcanoes in our data set that display significant temporal variation related to changes in state of activity.

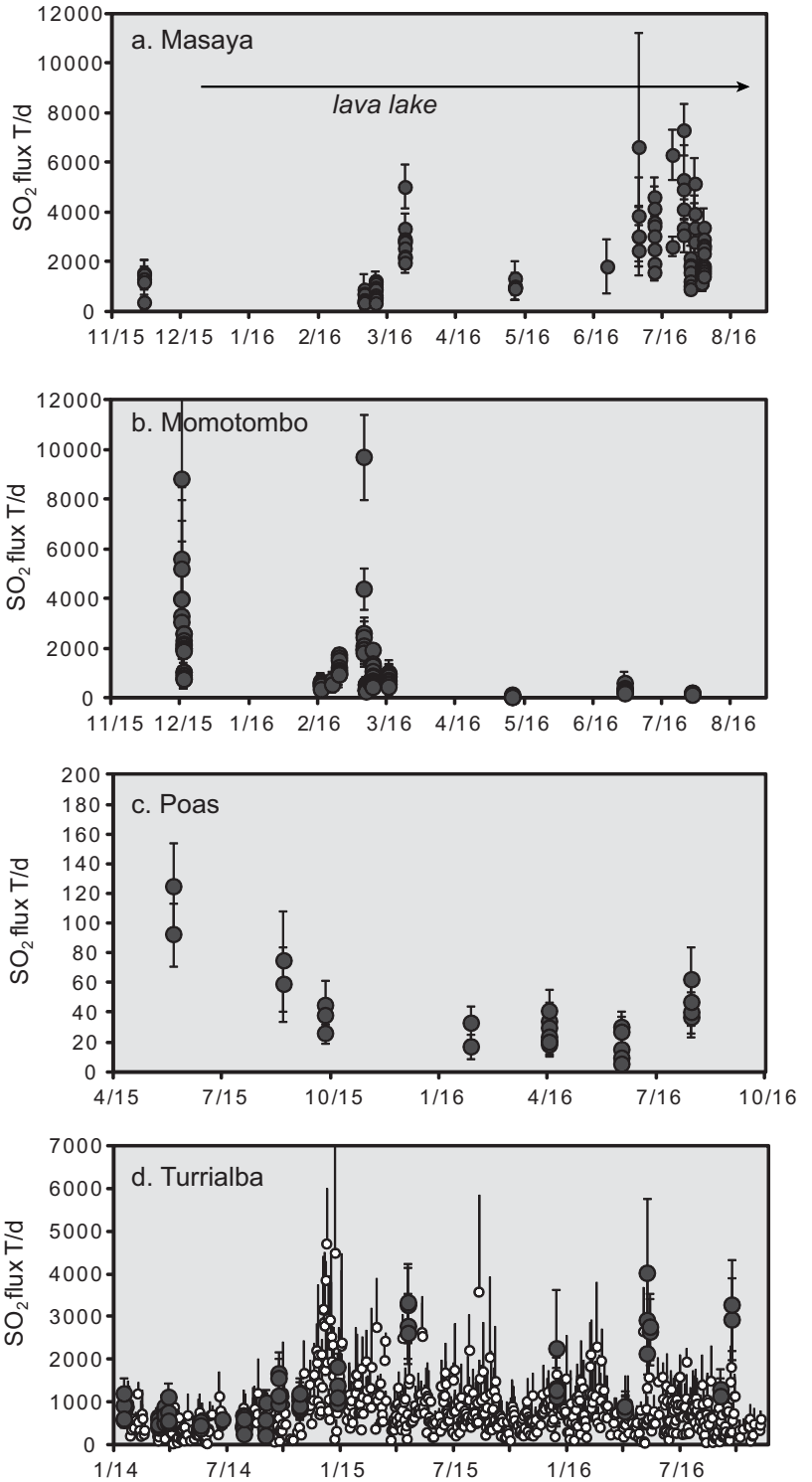

Figure 5. SO_2 flux time series for subset of volcanoes investigated. (a) Masaya volcano SO_2 fluxes showed a significant increase after appearance of the lava lake in December 2015. (b) Peak SO_2 fluxes at Momotombo were registered during eruptions, which ceased in April 2016 where after SO_2 fluxes attained a steady baseline. (c) Poás volcano displayed low SO_2 fluxes during the period of study. (d) Compares SO_2 fluxes from DOAS traverses (large grey circles) with scanning DOAS stations (small white circles) at Turrialba. Both data sets show an increase after October 2014, but near-real-time monitoring data from scanning DOAS significantly underestimate gas flux (see supporting information).

Prior studies (e.g., Andres & Kasgnoc, 1998) have taken a bimodal view of volcanic degassing and categorized degassing as either passive (implying constant low-flux) or eruptive (implying short-lived and high-flux during large magmatic eruptions). However, there is a broad spectrum of volcanic activity, from mild unrest without obvious surface expression, to phreatic eruptive activity, to sustained periods of low-energy ash emissions, to well-defined short-lived magmatic eruptive events of variable magnitude. Even passively degassing volcanoes can display significant variability in their gas output over short timescales. It is not trivial to define baseline degassing for most volcanoes without extensive time series data sets, and degassing behavior needs to be assessed on a volcano by volcano basis to determine what constitutes representative gas emission. In light of the diversity and sustained nature of volcanic activity at SCAVA, it is unreasonable to dismiss measurements conducted during prolonged periods of unrest as unrepresentative. Each volcano must be assessed individually to select only representative data to include in assessment of the S emission rate for the arc. This is an inherently imperfect exercise in which we have to make judgments based on field observations, experience in the field considering measurement conditions, and volcanic behavior. Ideally, with complete high-frequency, time-series data sets for all volcanoes, subjectivity would be eliminated. Though our data set is far larger than previous studies, we are still limited by incomplete time-series data.

Figure 5 shows time series plots of SO_2 flux data for selected volcanoes in our data set that show significant temporal variation. The average of all traverses conducted at Masaya (Figure 5a) yields an SO_2 flux of 2,270 T/d (n = 95; raw unfiltered averaged). Masaya has been a persistent strong gas emitter since SO_2 flux measurements were first conducted there in the 1970s (de Moor et al., 2013; Mather et al., 2006; Stoiber et al., 1986). The Santiago crater hosted a lava lake in the 1980s and 1990s. On 12 December 2015, a new, highly vigorous lava lake appeared, which persists to the time of writing. In our data set, a notable increase in SO_2 flux occurred in mid-June 2016, in which the average flux roughly doubled from 1,640 to 3,270 T/d. We also have more measurements conducted after this increase. Thus, taking a simple mean of daily average SO_2 flux would skew the value toward these more abundant measurements, resulting in an unrepresentative value for Masaya. Rather, we calculate a weighted mean value for the two periods 15 November 2015 to 15 June 2016 (213 days) and 15 June 2016 to 21 July 2016 (36 days), resulting in a value considered representative for our period of investigation of 1,880 $\pm$ 510 T/d. This value is far higher than the 800 T/d reported in Andres and Kasgnoc (1998) or the 867 $\pm$ 364 T/d reported in Carn et al. (2017), which we attribute to the heightened state of activity related to the recent appearance of the lava lake.

Momotombo volcano experienced a magmatic eruption that initiated on 1 December 2015 as Strombolian activity and continued until April 2016 as frequent Vulcanian explosions. Persistent degassing occurred between individual explosions. Our data set of DOAS traverses includes 108 measurements from Momotombo conducted in 2015 and 2016 (Figure 5b), showing a large range from 11,330 T/d to 150 T/d SO_2. A simple average of all SO_2 flux traverses yields 1,300 T/d; however some of these measurements were conducted during explosive events (fluxes >5,000 T/d on 2 December 2015 and 21 February 2016; see supporting information Table S1) and thus skew the average to an unrepresentative high value. Excluding data collected during explosive events shows that the background degassing during the eruptive period (December 2015 to April 2016) was 730 $\pm$ 230 T/d, here acknowledging that how "background" is defined depends on the time frame considered. Data collected after the eruptions ended in April 2016 show that degassing decreased to 290 $\pm$ 150 T/d. The weighted-mean value for persistent degassing at Momotombo for our period of measurements yields 540 $\pm$ 210 T/d, which is conservative because it does not include gas emitted during the initial eruption in early December 2015 or gas emitted during the frequent explosions in 2016 (n = 409; Global Volcanism Program, 2013). Based on data collected on 2–3 December 2015, we estimate that ~11 kT of SO_2 was emitted during the initial phase of the eruption (see supporting information section S2 and Figure S1). Similarly, data collected after a vulcanian blast on 21 February 2016 suggests that ~260 T of SO_2 was released by this event. Considering the total number of ash emission eruptions at Momotombo during 2015–2016, we estimate that the total eruptive SO_2 flux contributes the equivalent of ~75 T/d to the SO_2 flux inventory of Momotombo for 2015–2016, acknowledging that the errors in this estimation are very large (see supporting information). Nevertheless, the available data suggest that total amount of SO_2 emitted during discrete eruptive events was far lower than the amount of SO_2 emitted during persistent degassing between eruptions. Our estimation of 540 $\pm$ 210 T/d for baseline degassing based on 71 individual DOAS measurements during passive degassing (i.e., not explosive ejections of gas) at Momotombo during 2015–2016 is almost an order of magnitude higher than that of Andres and Kasgnoc (1998) of 75 T/d.

Telica volcano produced a sizeable vulcanian blast on 22 November 2015. Mobile DOAS traverses conducted the previous day failed to detect a measurable SO_2 plume. A few hours after the blast we conducted further DOAS traverses and measured SO_2 fluxes of 1,020 T/d to 1,300 T/d. Later measurements, conducted between April and July of 2016 indicate fluxes between 200 T/d and 360 T/d. Here, we dismiss the November 2015 measurements as nonrepresentative in the context of sustained degassing patterns as the lack of detectable SO_2 on 21 November 2015 suggest a blocked conduit, which was catastrophically opened by the eruption leading to release of accumulated volatiles and high SO_2 fluxes after the eruption. We do not have sufficient data to constrain the mass of SO_2 released during eruptions at Telica and assume this is minor compared to the persistent degassing flux. We thus only consider the data from April and July of 2016 and obtain an SO_2 flux for Telica of 270 ± 160 T/d.

The data series from San Cristobal volcano reveal a persistent degassing pattern over the study period. All of the data (other than the data from 25 April 2016 and some of the traverses from 16 July 2016 due to poor meteorological conditions) are therefore considered and the representative flux value is taken as the mean of the daily average emission rate measurements. Similarly, the few data available for Concepción and Rincón de la Vieja are accepted as representative in lieu of more extensive assessment, which is not possible with the currently available data.

All of the data from Nicaraguan volcanoes included in this study are from 2015 and 2016. Though many additional data are available for Costa Rican volcanoes from 2014, we only consider data from 2015 and 2016 (except for Rincón de la Vieja where no SO_2 flux data are available for 2015–2016, and Arenal where we include 2014 data) in order to provide a valid "snapshot" of the SCAVA.

Poás gas fluxes were relatively high (up to $\sim$500 T/d) during 2014 (de Moor et al., 2016b), and later declined drastically in 2015–2016 to $<$ 50 T/d (Figure 5c). Degassing at Poás consisted of two sources: the dome fumaroles, and the acid lake. Frequent phreatic eruptions occurred in 2014, which terminated in October. The SO_2 flux from the volcano later decayed slowly from average values of $>$200 T/d in 2014 to values of $<$50 T/d in early 2016. The changes in degassing character were dramatic, with the fumarole degassing decreasing from $>$150 T/d to less than 10 T/d, which was accompanied by a large decrease in fumarole temperature. Degassing from the acid lake decreased from a peak of $\sim$100 T/d in August to October 2014 to $\sim$15 T/d SO_2 in late 2015 to early 2016. The last measurements in the data set considered here (August 2016) showed a threefold increase in SO_2 flux from the lake, which was associated with the resumption of frequent phreatic eruptions between July and September 2016. Subsequent measurements in early 2017 showed very low SO_2 fluxes below the detection limit. SO_2 fluxes at Poás increased to $>$2,000 T/d after the April 2017 phreatomagmatic eruption. These large variations make the selection of a representative persistent gas flux challenging for this highly dynamic volcano. We consider all of the measurements between May 2015 and August 2016 to be representative of the state of degassing for 2015–2016, yielding a low SO_2 flux for Poás of 40 ± 30 T/d.

Turrialba entered a period of increased activity in October 2014. Before this escalation, SO_2 fluxes at Turrialba were between 350 and 1,300 T/d, with an average of about 650 T/d. The data considered in this study are again exclusively for the period 2015–2016. During this time SO_2 fluxes were high, as shown in Figure 5c, with daily averages ranging from 870 to 4,890 T/d, with a mean value of 2,600 $\pm$930 T/d. SO_2 flux in 2014 was in fact rather low in comparison with the years 2008–2013, and fluxes up to 3,500 T/d were measured in 2009 (Conde et al., 2013). The baseline before 2009 was considered to be around 350 T/d, but background fluxes were at least double that value in 2013. It is pertinent to note that the time series of Conde et al. (2013) suffered data gaps that missed the first three eruptive events at Turrialba in January 2010, January 2011, and January 2012. Campion et al. (2012) reported high SO_2 fluxes following the January 2010 eruption of $\sim$4,000 T/t and a slow decrease in SO_2 flux over the following months to values of around 1,500 T/d by the end of 2010.

Here, it is crucial to recognize the inherent differences in SO_2 measurement methods. The data from Conde et al. (2013) are from fixed scanning DOAS instruments, which probably yield underestimates of the SO_2 flux because the plume is often not scanned in its entirety, and also because no filtering was applied to these data to exclude cloudy days. On the other hand, Campion et al. (2012) base their time series of SO_2 degassing mostly on satellite measurements. In contrast to fixed scanning DOAS stations, these measurements may overestimate time-integrated SO_2 degassing because the detection limit for satellite-based

measurements is rather high and probably at least 500 T/d (depending on wind conditions and plume height; R. Campion, personal communication, 7 June 2017). Thus, days with low SO_2 flux are not recognized nor included in compilations of satellite measurements. At Turrialba, SO_2 fluxes may often be close to the detection limit for satellite measurements. Considering that scanning DOAS stations have measured SO_2 fluxes of well over 4,000 T/d at Turrialba on numerous occasions in 2015 and 2016, our daily average SO_2 fluxes for Turrialba ranging between 1,350 to 4890 T/d". Significant figures seem reasonable. Considering that ash emissions have been continuous and sustained for more than two years at Turrialba, it does not seem justifiable to exclude all data collected during extended periods of ash emissions as "anomalous." In the context of a decade of degassing at Turrialba, the increase in degassing since 2014 seems to be the next step in the evolution of the system toward ever increasing activity, and there are no signs that activity or degassing will decrease in the short or medium term. Thus, we include all of the Turrialba data for 2015–2016 as representative of the current and persistent state of degassing.

4.2. Gas Compositions

The compositions of gas emissions from 11 SCAVA volcanoes are presented in Tables 3 and 4. CO_2/SO_2, H_2S/SO_2 and H_2O/SO_2 are presented for Turrialba, Poás (fumaroles and lake gas emissions are distinguished; de Moor et al., 2016a), Rincón de la Vieja, Masaya, Cerro Negro, Telica, and San Cristobal. These compositions for actively degassing volcanoes were all measured by Multi-GAS in 2015–2016. Turrialba, Poás, and Masaya data come from a combination of permanent station data and campaign measurements. For comparison to these volcanoes, we also present data from volcanoes in a state of dormancy, namely Irazú and Arenal. Data are also presented for Las Pailas bubbling springs, which are located on the flanks of Rincón de la Vieja, and for Altomacis on the flanks of Tenorio. The emissions from dormant volcanoes do not contain SO_2 and data are presented as CO_2/H_2S, H_2/CO_2, and H_2O/CO_2.

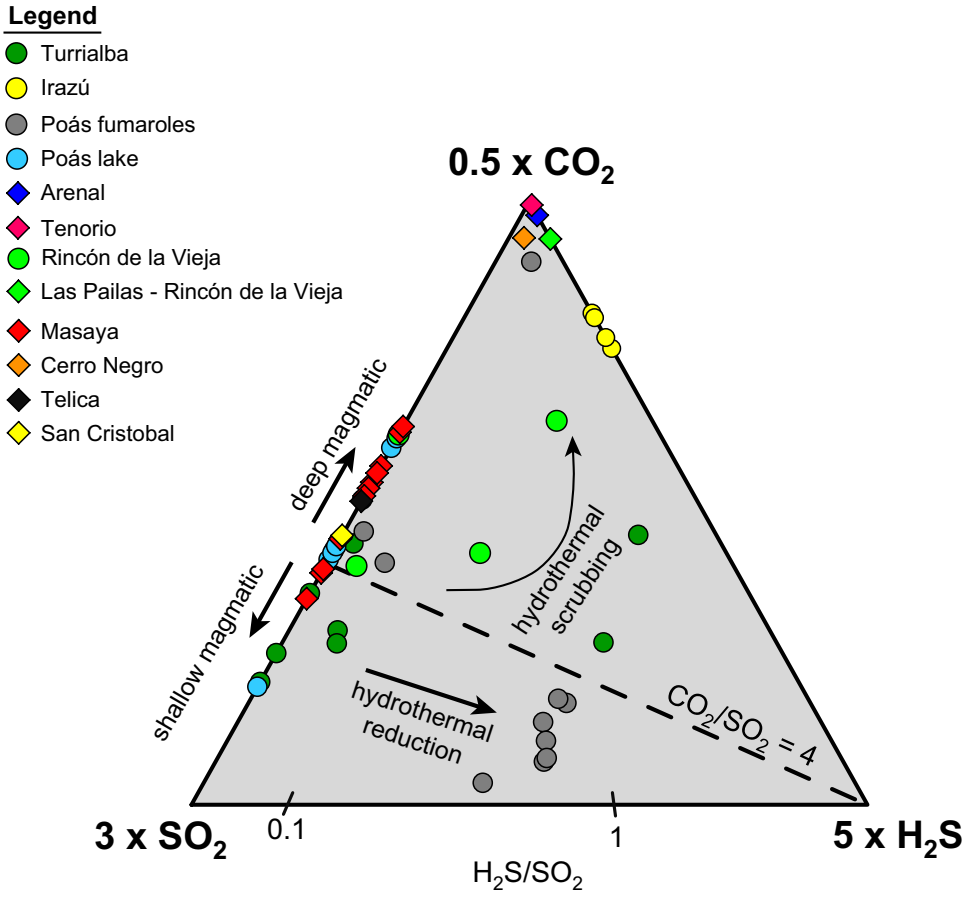

Figure 6. Triangular plot showing variations in SCAVA gas compositions in terms of CO_2, SO_2, and H_2S.

Figure 6 shows a triangular plot with gas compositions from the SCAVA volcanoes. Hydrothermal gases from dormant volcanoes plot near the CO_2 apex of the diagram and are poor in total sulfur, which is dominated by H_2S. Gas emissions from active volcanoes mostly plot close to the CO_2 – SO_2 axis and are poor in H_2S. Masaya, Telica, and San Cristobal gases contain no detectable H_2S and their average CO_2/SO_2 values for 2015–2016 are >4. Turrialba, Poás, and Rincón de la Vieja show more diverse gas compositions. These volcanoes have large hydrothermal systems as evidenced by the presence of crater lakes at Poás and Rincón de la Vieja, and the dominance of hydrothermal material in recent Turrialba ashes (Alvarado et al., 2016; de Moor et al., 2016a; Rizzo et al., 2016).

Three dominant processes modify surface gas emissions from their original magmatic composition. Hydrothermal scrubbing converts SO_2 to H_2S and $H_2SO_{4(aq)}$ by disassociation, removing S from the gas phase (e.g., Symonds et al., 2001). This process drives compositions away from the SO_2 apex and toward the H_2S and CO_2 apices, affecting gases from all of the Costa Rican volcanoes. The H_2S/SO_2 ratio in gases can also be modified without losing S from the gas phase by redox reactions during gas

cooling and interaction with hydrothermal systems (e.g., Giggenbach, 1987). Poás gases are most affected by sulfur reequilibration (Fischer et al., 2015) and plot toward the H_2S apex without S loss. Gas emissions from hyperacid crater lakes can be rich in sulfur (de Moor et al., 2016b; Tamburello et al., 2015). At Poás volcano emissions from the crater lake show variations in CO_2/SO_2 related to phreatic eruptions, and do not contain H_2S during periods of high gas flux (de Moor et al., 2016b). In the present data set, Poás crater lake emissions plot at oxidized compositions with relatively high CO_2/SO_2 compared to the data from 2014 (de Moor et al., 2016b). One data point from Rincón de la Vieja plots with the Poás crater lake compositions, consistent with similar hyperacid S scrubbing and oxidation processes at volcanoes with acid crater lakes.

Variations in magmatic degassing source also play a fundamental role in determining the gas compositions. In particular, deep magmatic degassing yields volcanic emissions with higher CO_2/SO_2 than shallow magmatic degassing, because CO_2 is less soluble than SO_2 in melts. Time series data sets from Turrialba (de Moor et al., 2016b) and Masaya (Aiuppa et al., 2017) show that variations in CO_2/SO_2 from these volcanoes are fundamentally controlled by deep versus shallow magmatic degassing. High CO_2/SO_2 is associated with new magma injection and is typically followed by increased volcanic activity and subsequent decrease in CO_2/SO_2. The temporal correlation between CO_2/SO_2 and eruptive activity in these mafic systems suggests that volatiles derived from deep injections of magma rise rapidly to the surface. Indeed, Ruprecht and Plank (2013) showed that Ni diffusion profiles in olivines at Irazú volcano in Costa Rica required magma transit times from the mantle to the surface on similar timescales to the eruptions (months to years). On the other hand, volatiles may be stored in crustal reservoirs or hydrothermal systems and remobilized during eruptions (e.g., Christopher et al., 2015; de Moor et al., 2005, 2016a; Oppenheimer, 1996), resulting in variations in gas emission compositions controlled by processes other than contemporaneous volatile exsolution from rising magmas. The consequences of dynamic changes in volcanic gas compositions on volatile budgets are poorly constrained.

The gas compositions observed in volcanic gas emissions also reflect margin-scale processes. Aiuppa et al. (2014, 2017) proposed that magmatic gases from the Nicaragua segment of SCAVA are richer in CO_2 than the Costa Rican segment of the arc, which they attributed to more efficient C release from the slab beneath Nicaragua. Our data set is compatible with this observation if only the most magmatic gas compositions are considered. Turrialba and Poás gases typically have $CO_2/SO_2 < 4$, whereas the Nicaraguan volcanoes show $CO_2/SO_2 > 4$ (Figure 6). Aiuppa et al. (2014) proposed that the division between Costa Rican and Nicaraguan arc segments fell at $CO_2/SO_2 \sim 3$, whereas our data suggests a slightly higher boundary at ~4. An increase in this division cutoff may suggest deeper magmatic gas sources along the arc in 2015–2016, here mostly due to higher CO_2/SO_2 observed at Turrialba and Masaya volcanoes in recent years. Alternatively, more efficient decarbonation from the downgoing slab or shallow crustal C assimilation could play a role in the higher CO_2/SO_2 ratios observed along the arc.

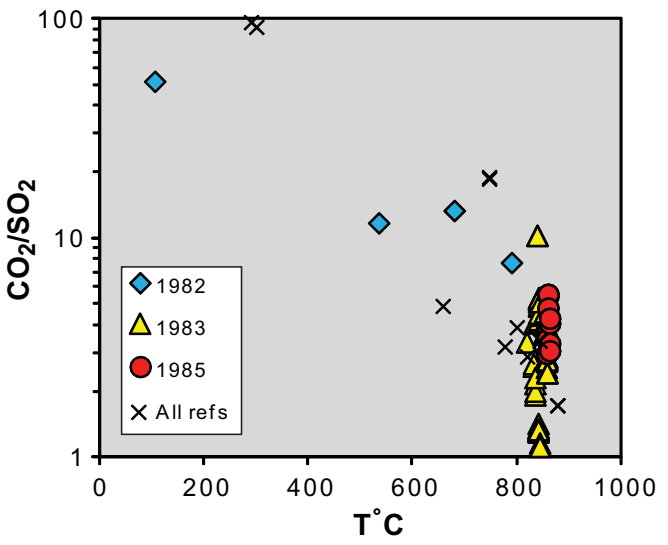

Figure 7. CO_2/SO_2 at Momotombo as a function of fumarole temperature. Data from Menyailov et al. (1986) are shown as filled symbols by sampling year. Other data are from Elkins et al. (2006), Giggenbach (1996), Symonds et al. (1994), Allard (1983), and Taran and Zelenski (2014).

In order to estimate total arc CO_2 fluxes based on the currently available data set, we pair gas compositions measured by Multi-GAS with SO_2 fluxes measured by mobile DOAS as closely as possible in time. The two largest gas emitters (Turrialba and Masaya) have good SO_2 flux and CO_2/SO_2 data sets, with gas flux and composition values generally paired to within a few hours or days. Poás volcano also has multiple contemporaneous SO_2 flux and CO_2/SO_2 measurements. Telica and San Cristobal volcanoes are somewhat less well constrained, with multiple SO_2 flux measurements but only one measurement of CO_2/SO_2 in the considered time period. For these volcanoes, the CO_2 flux is estimated for each daily average SO_2 flux using the single available CO_2/SO_2 ratio. Rincón de la Vieja has one contemporaneous measurement of SO_2 flux and CO_2/SO_2 from de Moor et al. (2016b). Within our data set, there are two cases in which gas compositions are not directly measured: we were unable to climb Momotombo volcano due to volcanic activity, and our

measurements of the plume at Concepción were undermined by heavy rain. The gas composition at Momotombo has been reported by Menyailov et al. (1986), Giggenbach (1996), Quisefit et al. (1989), Allard (1983), and Elkins et al. (2006). These studies measured complete gas compositions by direct sampling of high temperature fumaroles and a summary of gas CO_2/SO_2 as a function of fumarole temperature is shown in Figure 7. Fischer (2008) used a value of 3.4 for CO_2/SO_2 at Momotombo for calculating CO_2 flux, whereas Aiuppa et al. (2014) used a value of 2.9. We note that the lower temperature data trend toward the 1985 compositions measured by Menyailov et al. (1986) and that the 1983 values from one fumarole are anomalously low, perhaps due to sulfur remobilization. Here, we consider only the very highest temperature samples with $T > 850°C$, yielding an average CO_2/SO_2 value of 3.7 ± 0.9, which we assume in calculating the CO_2 flux for Momotombo in 2014–2015. No gas compositions are available for Concepción therefore we assume the average CO_2/SO_2 for the arc based on our data set, which is 5.1 (see below and Table 6).

Table 5
CO_2 Flux Estimates From SCAVA Volcanoes

Volcano	Date	CO_2 flux T/d	Error	n
Turrialba	29/12/2014	12,200	8,060	4
	22/4/2015	4,130	1,670	4
	18/12/2015	22,000	14,600	4
	6/4/2016	2,470	644	4
	12/5/2016	16,100	8,040	3
	17/5/2016	8,400	2,580	2
	8/9/2016	3,890	1,470	2
Poás	26/5/2015	109	25.0	2
	27/8/2015	67.0	29.4	2
	1/10/2015	36.3	10.3	3
	1/2/2016	24.9	10.5	2
	7/4/2016	26.8	10.5	7
	7/6/2016	16.8	7.3	6
	5/8/2016	46.5	16.1	4
Rincón de la Vieja	14/4/2014	312	193	10
Concepcion[a]	10/6/2015	102	92	5
	13/7/2016	185	241	3
Masaya	15/11/2015	7,860	2,300	5
	26/2/2016	6,160	1,440	11
	10/3/2016	13,900	2,790	9
	28/4/2016	4,880	2,480	5
	7/7/2016	10,300	1,670	2
	12/7/2016	13,100	1,940	6
	15/7/2016	4,150	893	7
	17/7/2016	11,400	1,630	4
	20/7/2016	4,350	1,330	12
	21/7/2016	11,300	2,820	10
Momotombo[a]	16/6/2016	950	622	6
	16/7/2016	511	202	6
Telica	24/6/2016	1,020	865	1
	16/7/2016	1,510	988	3
	17/7/2016	838	621	2
San Cristobal	10/6/2016	1,350	869	7
	24/6/2016	1,210	719	5
	14/7/2016	1,480	833	4
	16/7/2016	910	506	8
	17/7/2016	593	386	2
TOTAL ARC FLUX	2015–2016	22,500	4,940	182

Note. Daily SO_2 fluxes were determined from the mean of filtered data and paired with the closest measurement of CO_2/SO_2 in time to estimate CO_2 flux. Turrialba, Poás, and Masaya are well-constrained by multiple contemporaneous measurements, whereas Rincón de la Vieja, Telica, and San Cristobal have a single measurement of CO_2/SO_2 available for 2015–2016. Rincón de la Vieja data are from de Moor et al. (2016b) and gas compositions are assumed for Concepción and Momotombo. See text for details.

[a]No contemporaneous CO_2/SO_2 measurements available for these volcanoes. See text.

Table 6
Summary of Previous Arc Flux Estimates Compared to the Results of This Study

	Andres and Kasgnoc (1998) 1972–1997		Mather et al. (2006) 1997–2003		Aiuppa et al. (2014) 2013		This study 2015–2016	
SULFUR BUDGET	SO_2 flux T/d	±	SO_2 flux T/d	±	SO_2 flux T/d	±	SO_2 flux T/d	±
San Cristobal	590	NR	690	35%	181	35	334	147
Telica	84	NR	280	35%	64	34	269	160
Cerro Negro			NA	NA	NA	NA	0	2
Momotombo	73	NR	*73*	*NR*	*73*	*NR*	622	212
Masaya	790	NR	800	35%	*690*	*182*	1,880	510
Concepcion	NA	NA	NA	NA	NA	NA	39	41
Rincón de la Vieja	NA	NA	NA	NA	NA	NA	66	17
Arenal	110	NR	*180*	*35%*	NA	NA	0	3
Poás	500	NR	*8*	*35%*	124	30	47	32
Turrialba	NA	NA	NA	NA	754	214	2,990	980
TOTAL SO_2 OUTPUT	2,147		2,031	711	1,886	495	6,240	1,150

	Hilton et al. (2002); Shaw et al. (2003)		Mather et al. (2006)		Aiuppa et al. (2014)		This study	
CARBON BUDGET	CO_2/S_t	±	CO_2/SO_2	±	CO_2/SO_2	±	CO_2/SO_2	±
San Cristobal					4.2	1.3	4.8	1.9
Telica					3	0.9	6.1	2.7
Momotombo					*2.6*		3.7	0.9
Masaya			1.5–2.9	0.2	*2.6*	*0.7*	6.0	0.6
Concepcion							*5.1*	
Rincón de la Vieja					27	15.3	6.9	3.9
Poás					0.3	0.06	4.3	2.7
Turrialba					2.1	0.5	4.7	1.4
Weighted CO_2/SO_2 output	2.7		1.1–2.9		2.4		5.1	1.9
# of volcanoes considered	6		6		6		11	
% volcanoes measured	33%		17%		67%		82%	
TOTAL CO_2 OUTPUT	2,560–3,160		1,680–3,360		2,835 ± 1,364		22,500	4,940

Note. Values that were not measured in the relevant study but adopted from previous literature are shown in italics. NA = not analyzed, NR = not reported. Reported uncertainties (for 2015–2016) data in SO_2 flux are average error in DOAS measurements (Table 2) and uncertainties in CO_2/SO_2 are average error of linear regression fits (Figure 4).

4.3. Total Arc Volatile Fluxes

4.3.1. Comparison With Previous Studies

We achieve CO_2 flux estimates (Table 5) for each volcano by multiplying daily average SO_2 measurements with contemporaneous (in most cases) Multi-GAS measurements of CO_2/SO_2 (converted from molar to mass ratio). The time-averaged (2015–2016) gas fluxes for the volcanoes of SCAVA and our best estimate and uncertainties for the total volatile flux from SCAVA are presented in Table 6. Our survey yields total volatile fluxes of 6,240 ± 1,150 T/d SO_2 and 22,500 ± 4,940 T/d CO_2 from this 500 km section of arc. Our SO_2 flux for the total arc is a factor of 3 higher than any previous studies, and our CO_2 flux is almost an order of magnitude higher than previous studies, as summarized in Table 6.

Before proposing reasons for our higher volatile fluxes, previous estimates and methods need to be reviewed to assess whether direct comparisons between our data and previous studies are appropriate. Hilton et al. (2002) and Shaw et al. (2003) used the SO_2 flux data set of Andres and Kasgnoc (1998; in which fluxes for six volcanoes in SCAVA reported) combined with direct samples from high T fumaroles to estimate the CO_2 flux. These studies considered a CO_2/S_T (where $S_T = SO_2 + H_2S$) of 2.7 as the composition of the bulk arc output for Central America, including Mexico (El Chichón), based on the median value of gas samples (n = 93) collected from fumarole and bubbling springs. This median value is dominated by the

high temperature samples from Momotombo (Menyailov et al., 1986) with 47 samples and an average value of 2.2. In these calculations, the high temperature Momotombo value was regarded as most representative of the magmatic value and least affected by shallow processes that affected the CO_2/S_T ratios of the majority of the other data. Combining SO_2 flux with CO_2/S_T rather than CO_2/SO_2 to estimate CO_2 flux was reasonable at the time, with the assumption that H_2S oxidizes quickly upon contact with air. Later work has shown that H_2S oxidation in air is kinetically inhibited and is relatively stable in volcanic plumes (Aiuppa et al., 2005). This is supported by the fact that H_2S is clearly measurable by permanent Multi-GAS; for example, in the Turrialba plume at a distance of a few hundred meters from the vents (de Moor et al., 2016a).

It is important to note that both gas compositions and fluxes vary dramatically at SCAVA volcanoes, as has been demonstrated in above sections. Thus, combining gas compositions with SO_2 fluxes measurements that were not conducted at the same time is likely to produce spurious estimates of total arc flux. The Hilton et al. (2002) and Shaw et al. (2003) work certainly suffer from this problem. For example, an SO_2 flux of 500 T/d was reported for Poás by Andres and Kasgnoc (1998). In contrast, the SO_2 flux at Poás was measured at just 8 T/d by Zimmer et al. (2004) and these measurements were conducted at the same time as samples were taken for $CO_2/^3He$ at Poás. Using time-averaged (several decades) fluxes of SO_2 combined with time average CO_2/SO_2 is expected to overcome some of these issues.

Shaw et al. (2003) compared their CO_2 flux estimate from Andres and Kasgnoc (1998) COSPEC measurements (fluxes for 6 SCAVA volcanoes reported) with a CO_2 flux derived from the global ^3He flux estimated from arcs scaled to the arc length of CAVA (Costa Rica to Guatemala) and $CO_2/^3He$ in a subset of their samples from Costa Rica and Nicaragua. The global ^3He flux from arcs is however only roughly estimated by: (1) assuming the arc ^3He flux composes 20% of the ^3He flux from MORB (Torgersen, 1989); (2) scaling ^3He flux to the CO_2 flux estimated for arc volcanoes based on a small number of actual measurements (Allard, 1992); or (3) by using gas ratios (essentially $^3He/SO_2$) and the SO_2 flux (Hilton et al., 2002; Marty et al.,1989; Marty & LeCloarec, 1992). The uncertainties in using the ^3He flux to derive CO_2 flux are difficult to quantify making comparisons to other methods challenging. Considering the fact that estimates of the global ^3He flux from arcs is in part derived from SO_2 and CO_2 flux measurements, it is a circular argument to use the global ^3He flux scaled down to an arc segment to subsequently estimate CO_2 flux. Furthermore, these estimates rely heavily on the choice of $CO_2/^3He$ values used. Many of the samples used in the Shaw et al. (2003) estimation of the arc $CO_2/^3He$ come from low temperature geothermal features, and phase separation processes can greatly affect these values (e.g., Barry et al., 2013 and references therein), though this was not considered in Shaw et al. (2003). Magma degassing can also fractionate CO_2 from ^3He based on their different solubilities in melt such that $CO_2/^3He$ decreases with degree of magmatic degassing (Barry et al., 2014 and references therein). Direct measurement of ^3He anomalies in air could present a future method to directly measure ^3He fluxes from subaerial volcanoes; however, extremely high analytical precision is needed to detect small variations in $^3He/^4He$ in air (Boucher et al., 2017).

Later studies estimated SO_2 and CO_2 fluxes based on flux measurements at fewer volcanoes than reported in Andres and Kasgnoc (1998), and validated their estimations by comparison with the Hilton et al. (2002) and Shaw et al. (2003) studies. Mather et al. (2006) measured SO_2 fluxes at Masaya, Telica, and San Cristobal (total number of transects = 23) and compiled further data from the literature to estimate total arc fluxes for the CAVA (Costa Rica to Guatemala). It is impossible to compare uncertainties between the Mather et al. (2006) study and the Andres and Kasgnoc (1998) study because the latter did not present errors or data for individual COSPEC transects. Mather et al. (2006) attempted to compare arc SO_2 fluxes for the periods 1997–2003 to 1972–1997 (i.e., the Andres and Kasgnoc (1998) study) reporting similar total arc fluxes in the two periods. Mather et al. (2006) measured gas compositions at Masaya by FTIR and calculated gas fluxes for the entire CAVA based on Masaya gas compositions. They assumed a power law distribution of SO_2 fluxes (Brantley & Koepenick, 1995), acknowledging that this method was prone to large uncertainties.

The major problem with combining purely magmatic gas compositions such as those measured at Masaya with SO_2 fluxes measured at multiple volcanoes in various states of degassing is that CO_2/SO_2 may be vastly underestimated for degassing volcanoes with hydrothermal systems because S scrubbing or reduction is a ubiquitous process in these systems (Figure 6). Even high SO_2 fluxes can be associated with high CO_2/SO_2

Table 7
Comparison of Daily Average Mobile DOAS Data With Scanning DOAS Station Data for Turrialba Volcano

	Mobile DOAS T/d	± T/d	Scanning DOAS T/d	± T/d	Mobile/Scanning
de Moor et al. (2016a)					
1/18/2014	830	290	na	na	na
3/15/2014	520	120	190	40	2.76
3/25/2014	720	160	150	20	*4.96*
3/31/2014	670	240	720	190	0.93
5/22/2014	450	80	580	230	0.78
6/26/2014	590	na	510	110	1.15
7/30/2014	490	130	870	270	*0.56*
7/31/2014	470	190	500	110	0.93
9/4/2014	350	150	440	150	0.81
9/5/2014	990	na	480	140	2.05
9/25/2014	1,330	340	630	190	2.12
10/29/2014	1,000	150	360	120	2.79
			Average ratio:		1.59
			Std dev.:		0.84
This study					
29/12/2014	2,810	630	1,270	460	2.21
22/04/2015	3,910	1,060	1,150	360	3.40
18/12/2015	1,810	1,100	1,650	550	1.10
06/04/2016	1,720	270	1,040	440	1.67
12/05/2016	4,890	2,100	1,130	440	4.32
17/05/2016	3,770	1,000	740	220	*5.08*
08/09/2016	1,350	500	550	140	2.47
26/09/2016	4,840	1,810	680	170	*7.14*
			Average ratio:		2.17
			Std dev.:		1.06

Note. The correction factor (Mobile/Scanning) is presented for each day, and the average and std deviation reported for before and after the 29 October 2014 eruption. Numbers in italics were considered anomalous and not used in the mean.

and H_2S/SO_2 ratios, as was recently demonstrated at Turrialba (de Moor et al., 2016a). On the other hand, a decrease in SO_2 flux is often associated with an increase in CO_2/SO_2 as increasing hydrothermal interaction removes S from the gas phase. The Hilton et al. (2002), Shaw et al. (2003), and Mather et al. (2006) estimates of CO_2 flux from SCAVA all apply purely magmatic CO_2/SO_2 values (i.e., low values) based on few data points to the entire arc segment.

The latest compilation of gas flux measurements for the SCAVA is reported in Aiuppa et al. (2014), who focused on Multi-GAS measurements of SCAVA volcanoes but also reported SO_2 flux at Turrialba, Poás, Telica, and San Cristobal volcanoes in 2013. This study calculates CO_2 flux for these volcanoes based on actual plume-composition measurements combined with contemporaneous SO_2 flux estimates, representing an improvement over previous estimates. The SO_2 fluxes estimated for these volcanoes were based on NOVAC-style scanning DOAS instruments at Turrialba, Telica, and San Cristobal. These scanning measurements are intrinsically subject to larger uncertainties than vertical pointing DOAS traverses because knowledge of the plume height and/or distance must be known in order to estimate plume width (Galle et al., 2010). Thus, errors in plume position translate proportionally to errors in SO_2 flux.

Comparison between our vertical DOAS transects and scanning DOAS measurements at Turrialba (Figure 5 and Table 7) indicate that SO_2 flux from scanning DOAS underestimates the SO_2 flux at Turrialba by a factor of 1.6 in 2014 (de Moor et al., 2016a), and a factor of 2.2 in 2015–2016 (this study). A detailed assessment of scanning DOAS versus DOAS traverse measurements, and how to improve scanning DOAS accuracy at Turrialba, is provided in the supporting information section S3 and Table S4. The Aiuppa et al. (2014) estimates for SO_2 fluxes from San Cristobal and Telica are similarly low compared to previous estimates based on traverse data (Figure 8). Furthermore, the Aiuppa et al. (2014) study determined the SO_2 flux for Poás by

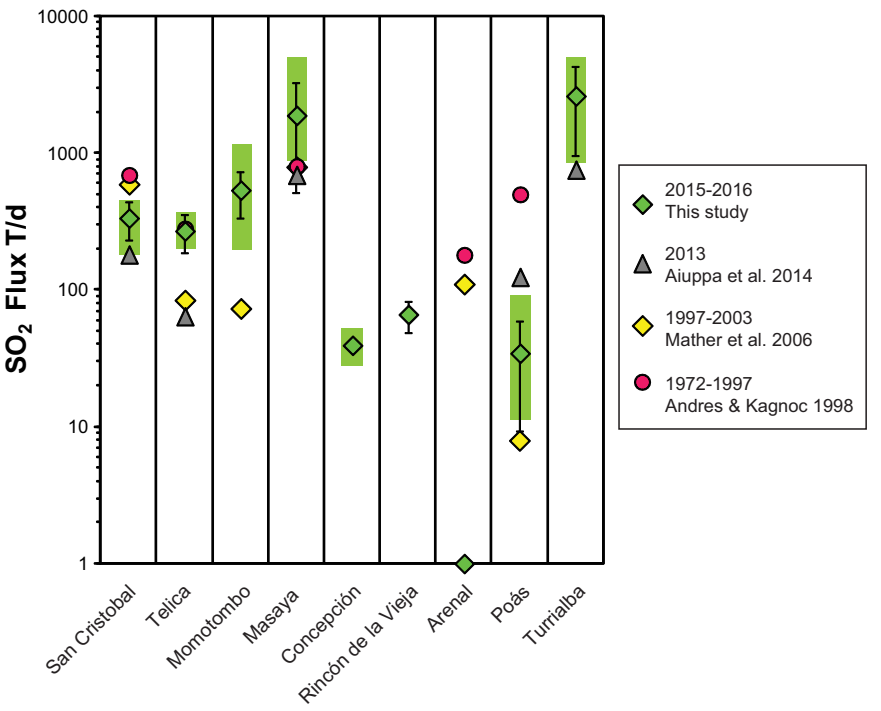

Figure 8. Flux estimate comparisons for SCAVA volcanoes compared with previous studies (Aiuppa et al., 2014; Andres & Kasgnoc, 1998; Mather et al., 2006). The error bars on the 2015–2016 data are 1 standard deviation about the mean (green diamonds) and the green-shaded rectangles represent the range in the SO2 flux estimates for each volcano.

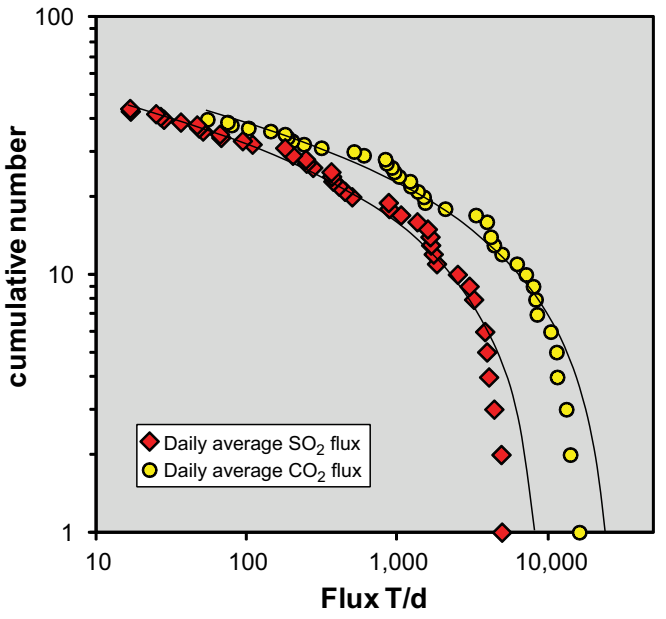

Figure 9. Cumulative number of daily average flux values versus gas flux, showing statistical distribution for SCAVA SO_2 and CO_2 fluxes in 2015–2016. Neither SO_2 nor CO_2 fluxes follow a power law, which would plot as a straight line. Rather, natural logarithm curves (SO_2: $y = -7.1\ln(x) + 65.1$; $R^2 = 0.987$. CO_2: $y = -6.9\ln(x) + 70.6$; $R^2 = 0.978$) seem a better fit to the data, though the fit is less good at higher flux values.

walking traverse for the dome fumaroles only. However, de Moor et al. (2016b) show that the acid lake is also an important contributor to SO_2 and CO_2 emissions at Poás. Therefore, the SO_2 flux data presented in Aiuppa et al. (2014) seem to be significantly underestimated. In contrast to previous compilations of gas fluxes for SCAVA, Aiuppa et al. (2014) did not assume a power law distribution to infer fluxes from unmeasured volcanoes.

Similar to the Aiuppa et al. (2014) study, our estimate of the gas flux from SCAVA is a minimum estimate and also relies on incomplete data. First, we are forced to use NOAA wind speed data, with a calibration by anemometer measurements (affected by local topography) conducted at volcano summits. However, our limited dual vertical DOAS measurements (conducted downwind and at the same distance from the volcanoes as DOAS traverses of the two largest SO_2 emitters: Turrialba and Masaya) suggest that both NOAA and anemometer methods underestimate plume speeds by as much as 30%. Further study is needed in this area and future studies should clearly present how plume speeds were determined and the associated errors. Second, most radiative transfer effects tend to underestimate true SO_2 column densities. Light dilution and strong UV absorption at low wavelengths both lead to underestimation of SO_2 column amounts, whereas plume scattering is the only artifact known to increase apparent SO_2 column amounts (Kern et al., 2010). Third, we have excluded some high gas fluxes measured during eruptive activity (e.g., Telica) as well as data for some of the peak degassing events at Turrialba. Fourth, we have thus far only considered active degassing volcanoes

with SO_2 plumes and have not considered diffuse degassing of CO_2 or H_2S at dormant volcanoes. To date, measurements of diffuse degassing in SCAVA are few and dominated by work close to volcanoes (e.g., Lucic et al., 2014), and yet, CO_2 flux over broad geographic area in arc settings may also be significant (Chiodini et al., 2003).

4.3.2. Statistical Distribution of Degassing Volcanoes

Previous estimates of global and regional volatile fluxes from volcanoes have employed various methods of extrapolation to extend limited data sets to include unmeasured volcanoes. Here, we consider the statistical distribution of degassing at SCAVA for 2014–2015 based on our data set.

Figure 9 shows cumulative frequency-flux distribution following Brantley and Koepenick (1995) and Mori et al. (2013). Brantley and Koepenick (1995) proposed that volcanic subaerial flux distribution may follow a power law, or fractal pattern. We consider daily average SO_2 ($n = 45$) and CO_2 ($n = 42$) fluxes from eight SCAVA volcanoes, following Mori et al. (2013) who considered 6 month-average SO_2 fluxes for the Japanese arc. The data shown in Figure 9 exclude data with poor measurement conditions or fluxes associated with short-lived eruptive events (sections 4.1.1 and 4.1.2). The SCAVA volcanoes do not follow a power law distribution, which would plot as a straight line on the cumulative frequency-flux plot. Rather, a "roll-over" distribution occurs similar to that for the Japanese volcanoes. Interestingly, the changes in slope for the SCAVA distribution seem to occur at similar flux values to the Japanese volcanoes, with a change in slope occurring at 300–500 T/d and another at ~2,000 T/d (excluding Miyakejima in the Japanese data set). The volcanological reason for this remains unclear. Figure 9 shows that based on our data set CO_2 flux follows a similar distribution pattern to SO_2 flux. Both distributions are better fit with a natural logarithmic curve than with a power law.

If a widely applicable statistical distribution pattern were verified, then contemporaneous measurement of the SO_2 or CO_2 flux from the 20 (of ~150 actively degassing volcanoes worldwide) largest emitters of volcanic volatiles could be sufficient to infer the flux from all other actively, passively, and cryptically degassing volcanoes on Earth at any given time (Brantley & Koepenick, 1995). Efforts to quantify global arc volatile fluxes have embraced the power law approach (e.g., Fischer, 2008; Hilton et al., 2002). Similarly, volatile fluxes from the CAVA arc have also used power law extrapolation to account for unmeasured volcanoes (Mather et al., 2006; Shaw et al., 2003). Mori et al. (2013) recently showed that based on data from 22 Japanese volcanoes monitored between 1975 and 2006, the flux distribution did not follow a power law. Rather, they found that measuring roughly the top third of the emitters approximates the total regional SO_2 and further extrapolation based on power law was not valid. In a very different approach, Burton et al. (2013) used a linear extrapolation to extend their compilation of 33 volcanoes with measured CO_2 fluxes to the 150 active volcanoes on Earth. Using this approach, they extrapolated from a measured volcanic CO_2 flux of 60 Mt/yr to an estimated global CO_2 flux of 270 Mt/yr, which gives a far higher estimation of global flux than assuming a power law to extrapolate to only the unmeasured low-flux volcanoes. The approach of Burton et al. (2013) was justified by the assertion that there remain large unmeasured CO_2 emitters (4–5 times more than have been measured) that are unaccounted for in the existing data.

4.3.3. Temporal and Spatial Distribution of Arc Degassing

The ultimate goals of estimating the total flux of S or C from global or regional volcanoes are to gain insight into global element cycles and to relate variations in flux to tectonic or volcanic activity. A significant challenge is to establish whether the bulk Earth is "ingassing" or "outgassing" i.e., whether there is net gain or loss of S or C from surface reservoirs to deep reservoirs. Here, we address some of the details of the approaches and outstanding questions implicit in this fundamental problem.

Many previous studies have suggested that persistent, passive-degassing volcanoes dominate the global flux of SO_2 (and other volatiles) to the atmosphere, and that instantaneous high-flux events (i.e., eruptions) are a minor contributor that can essentially be ignored from the global degassing budget (e.g., Andres & Kasgnoc, 1998; Carn et al., 2017; Hilton et al., 2002; Shinohara, 2013). This approach views volcanic behavior as consisting of two extreme end-members only, namely constant persistent degassing with punctuated near-instantaneous events releasing bursts of gas. However, the spectrum of volcanic activity is diverse and dynamic and temporal variations in degassing behavior may dramatically change volatile budgets for arcs. The effects of volatile solubility on the relative contributions of passive degassing versus eruptive degassing have not been addressed.

The Japanese arc and SCAVA provide prime examples, as these have comparatively good time-series data in the global data set. Mori et al. (2013) showed that the activation of Miyakejima volcano greatly affected the

volatile budget for the Japanese arc. The total time-averaged SO_2 flux for the arc for 1975–2006 was 6,013 T/d for the ~1,400 km length of the arc segment. Miyakejima activated in 2000, yet its time averaged SO_2 flux for 1975–2006 was 2,119 T/d or about a third of the total arc flux. Clearly, if the period for time integration were shortened to 2000–2006 the contribution from Miyakejima would be even more disproportionate.

Similarly, the activation of Turrialba volcano in the early 2000s dramatically changes the estimate of volatile output from SCAVA. In this study, we have taken the approach to present a "snapshot" of the arc segment, using only data that were collected and processed with an internally consistent methodology (i.e., vertical pointing DOAS traverses, using "calibrated" NOAA wind speed). Our data are therefore limited to the period 2015–2016, since all of the data from Nicaragua were collected during this time. Of the total SO_2 flux from SCAVA (6,240 ± 1,150 T/d) Turrialba volcano currently represents ~48% (2,990 ± 980 T/d) of the total flux. This reactivation clearly does not fit the extreme end-members often considered for volcanic degassing; i.e., either persistent degassing or very short-lived bursts of gas during paroxysmal eruptions. Turrialba has now been a major contributor to the SCAVA gas budget for a decade. If we consider that the instrumental record of arc-scale volcanic degassing extends back to the mid-1980s (though this is rather generous—see section 4.3), Turrialba has been actively degassing for about a quarter of that time. Indeed, the contribution of Turrialba to the total arc flux appears to be increasing with time and there are no indications that activity will decrease in the near future. Nevado del Ruiz in Colombia and Popocatépetl in Mexico are other examples of volcanoes that reactivated and thereafter entered patterns of variable persistent degassing with frequent eruptions. Indeed, volcanic degassing behavior is clearly not limited to constant persistent degassing or instantaneous gas bursts.

Prior to the reactivation of Turrialba, Masaya strongly dominated the total gas budget of SCAVA, representing 35–40% of the total arc SO_2 flux. Our estimate of Masaya degassing (1,878 ± 511 T/d) is higher than previous estimates, and represents 30% of our total flux for SCAVA for 2015–2016. Interestingly, many of our estimates for individual volcanoes are higher than previous studies (see Figure 8). A notable exception is Arenal volcano, which returned to quiescence in 2010 after a 40 year-eruption period (note that Arenal SO_2 flux is probably significantly underestimated in previous compilations because the only data available are from Williams-Jones et al. (2001), who used wind speeds measured ~1,000 m below the volcano summit).

The dominance of volcanoes like Masaya, Miyakejima, Popocatépetl, and Turrialba in regional volatile budgets raises important questions about the spatial distribution of volatile outgassing versus ingassing at arcs on the regional scale. Volcanoes must provide an outlet for release of volatiles from the slab (and shallower sources) liberated from a relatively isolated downgoing section of the slab. For example, Masaya volcano probably samples fluids released from a ~70 km arc-length segment (half the distance between Momotombo and Concepción), or about 13% of the total length of SCAVA (535 km), yet contributes a time-averaged SO_2 flux of about 35% of the arc. Either there are extreme along-arc spatial heterogeneities in the ratio of volatiles subducted to volatiles outgassed, or there must be dramatic short-term variations (on geologic timescales) in gas flux along-arc. Taking these variations into consideration presents a major challenge to establishing whether the bulk Earth is ingassing or outgassing on any timescale relevant to the bulk Earth system based on existing measurements of volcanic-gas fluxes.

4.3.4. Comparison With Arc Inputs

The most detailed calculation of volatile inputs to the Central American subduction zone to date were conducted by Freundt et al. (2014). This study considered S and C inputs to the subduction zone from subducted sediments, igneous oceanic crust, serpentinized mantle, and eroded material from the overlying plate. Here, we follow the approach of Freundt et al. (2014) with minor modifications in assessing the volatile inputs to SCAVA. The input budgets of sulfur and carbon for the Nicaraguan and Costa Rican arc segments are presented in Table 8. There are important distinctions between subduction input compositions in the slabs at Nicaragua versus Costa Rica, which may play an important role in determining variation in arc outputs. Alternatively, physical (rather than chemical) differences in subduction parameters (slab temperature, slab dip) may play important roles.

The sedimentary section subducted in Costa Rica and Nicaragua is essentially the same, consisting of ~150 m of hemipelagic clays overlying ~250 m of pelagic carbonates. The bulk S and CO_2 concentrations of the sediments are 0.2 and 27 wt.%, respectively (Table 8). The oceanic igneous crust is thicker offshore Costa Rica in comparison to that of Nicaragua due to the presence of the Cocos ridge and abundant seamounts (Figure 1). We follow Freundt et al. (2014; and references therein) and accept an igneous crustal

Table 8
Arc Input Budgets of S and C for the Nicaraguan and Costa Rican Arc Segments, Modified From Freundt et al. (2014)

		NICARAGUA					COSTA RICA					SCAVA
	Units	Seds	Ign Crust	Serp mantle	Erosion	Subtotal	Seds	Ign Crust	Serp mantle	Erosion	Subtotal	TOTAL
Length[a]	km	276	276	276	276		264	264	264	264		
Velocity	mm/y	71	71	71	na		76	76	76	na		
Thickness	m	400	5,000	7,000	na		400	7,000	3,000	na		
Density	kg/m3	1,620	2,930	3,000	2,930		1,620	2,930	3,000	2,930		
Vol flux	m3/y	7.8E+06	9.8E+07	1.4E+08	8.3E+06		8.0E+06	1.4E+08	6.0E+07	3.0E+07		
Mass flux	kg/y	1.3E+10	2.9E+11	4.1E+11	2.4E+10		1.3E+10	4.1E+11	1.8E+11	8.7E+10		
S budget												
S conc[b]	wt%	0.21	0.10	0.02	0.10		0.21	0.10	0.02	0.10		
S flux	kg/y	2.7E+07	2.9E+08	8.2E+07	2.4E+07		2.7E+07	4.1E+08	3.6E+07	8.7E+07		
SO_2 flux	T/d	146	1,580	451	133	2,300	150	2,260	198	479	3,100	5,400
% contrib		6	68	20	6		5	73	6	16		
C budget												
CO_2 conc	wt%	26.6	0.18	0.02	0.54		26.6	0.18	0.02	0.54		
CO_2 flux	kg/y	3.4E+09	5.2E+08	8.2E+07	1.3E+08		3.5E+09	7.4E+08	3.6E+07	4.7E+08		
CO_2 flux	T/d	9,240	1,420	225	359	11,200	9,460	2,030	99	1,290	12,900	24,100
% contrib		82	13	2	3		73	16	1	10		
CO_2/SO_2 molar		91.9	1.3	0.7	3.9	7.1	91.9	1.3	0.7	3.9	6.1	6.5

[a]We calculate arc length based on distance between active volcanoes rather than trench length as used by Freundt et al. (2014) as we consider the source region sampled by the degassing arc from San Cristobal to Turrialba. Hence, our arc lengths are slightly less than those of Freundt et al. (2014) who also considered the entire trench length from Consiguina to the north and southern Costa Rica where there are no degassing volcanoes.
[b]Our S concentration for the bulk sedimentary section is slightly higher than that used by Freundt et al. (2014) because we include 200 ppm sulfate in the carbonate units after Burdett et al. (1989).

thickness of 7 km off Costa Rica, versus 5 km off Nicaragua. The S and CO_2 concentrations are 0.1 and 0.18 wt.%, respectively (Freundt et al., 2014). The serpentinized mantle is more prolific in Nicaragua than in Costa Rica, due to trench-parallel faulting in response to slab bending. These faults penetrate to mantle depths off Nicaragua, providing fluid pathways resulting in serpentinization of mantle peridotite (Ranero et al., 2003; Ranero & Weinrebe, 2005). Thickened crust off Costa Rica does not favor slab bending, therefore less serpentinized mantle is thought to be present. Serpentinites tend to have S contents of 0.08–0.4 wt % (Alt et al., 2007, 2012) and 0.006–0.3 wt.% CO_2 (Alt et al. 2013). We follow Freundt et al. (2014) adopting a 7 km thick mantle lithosphere that is 10% serpentinized, with a bulk S concentration of 0.02 wt.% as well as 0.02 wt.% CO_2. In Costa Rica, the serpentinized mantle is only 3 km thick. Subduction erosion of the overlying plate is more efficient in Costa Rica, where the subduction of the buoyant and rough seamounts province takes place resulting in an estimated flux of crustal material of 113 versus 12 km^3/Ma/km in Nicaragua (Freundt et al., 2014; Vannucchi et al., 2003, 2004). The eroded material has a composition similar to altered oceanic crust, with ~0.1 and 0.54 wt.%, S and CO_2, respectively (Freundt et al., 2014).

Interestingly, the CO_2/SO_2 molar ratio of bulk subduction zone inputs is higher in Nicaragua than in Costa Rica (Table 8), mimicking the higher CO_2/SO_2 ratio observed in Nicaraguan gas emissions. Using these inputs from the literature, we estimate the total fluxes of sulfur and carbon into the SCAVA subduction zone as ~5,400 T/d SO_2 and ~24,000 T/d CO_2. These input fluxes are within uncertainty of the estimated output fluxes from SCAVA for 2015-–2016.

Whereas the fluxes of sulfur and carbon into the SCAVA subduction zone appear to be very similar to the degassing fluxes of these volatiles from active volcanism in 2015–2016, the sources and processes involved in subduction zone volatile cycles are complex and strongly debated. Carbon devolatilization or mobilization by fluid-mediated reactions or slab melting is complex (e.g., Ague & Nicolescu, 2014; Duncan & Dasgupta, 2017; Tumiati et al., 2017) and likely results in fractionation of carbon from sulfur. Other sources of volatiles at arc volcanoes include volatiles assimilated from lithologies in the overriding plate (e.g., Troll et al., 2012), magmatic or hydrothermal volatiles stored in crustal or mantle reservoirs for poorly defined

periods of time (e.g., Christopher et al., 2015; de Moor et al., 2016a; Oppenheimer, 1996), and the mantle wedge (e.g., Scambelluri et al., 2016). It remains a matter of debate whether subduction zones represent a net gain or net loss of carbon to the deep mantle (e.g., Kelemen & Manning, 2015; Mason et al., 2017; Thomson et al., 2016), a key objective of Deep Carbon Observatory research. A key quantitative and directly measurable (yet still under constrained) parameter for assessing the net gain or loss of CO_2 to surface reservoirs at subduction zones is the global volcanic gas flux.

4.3.5. Volatile Budget of the Southern Central American Subduction Zone

Our estimate for SO_2 degassing output from SCAVA active volcanoes in 2015–2016 is 6,240 ± 1,150 tons/d or $3.56 \times 10^{10} \pm 0.65 \times 10^{10}$ mol/yr. Combining our SO_2 flux data set with Multi-GAS CO_2/SO_2 values measured at the same time, we estimate the 2015–2016 CO_2 flux from active volcanic degassing at SCAVA to be 22,500 ± 4,940 T/d or $1.87 \times 10^{11} \pm 0.41 \times 10^{11}$ mol/yr.

At first inspection, these outputs appear remarkably similar to the arc inputs. The S inputs and outputs to the arc are within error of one another. Similarly, the estimated CO_2 flux from the arc is within error of the total carbon input. It is further notable that the C/S of inputs and outputs are similar (6.5 versus 5.3, respectively). A simplistic interpretation of the data would therefore be that all of the subducted S and C is efficiently recycled to the surface through arc degassing. However, other considerations must be taken into account before drawing such a conclusion.

First, the mantle is a major source of volatiles in arc gas emissions. The data presented in this work do not allow calculation of the contribution of mantle versus crustal (either subducted crust or assimilated upper-plate crustal volatiles). Previous studies based on $CO_2/^3He$ and $\delta^{13}C$ in gases (Shaw et al., 2003) have concluded that the dominant source of C in SCAVA emissions is subducted material, with the minor proportion of mantle carbon being between 5% and 10%. This method suggests that limestone carbon is the dominant contributor, at 70%–95%. Interestingly, Shaw et al. (2003) suggested that C recycling at the SCAVA arc was particularly inefficient compared to global arcs. If we assume that the mantle contribution to carbon emissions from SCAVA remains relatively constant through time, then our data suggest the opposite—that C recycling was extremely efficient during our 2015–2016 survey period. However, uncertainties remain in whether $\delta^{13}C$ and $CO_2/^3He$ are faithful recorders of source characteristics. Recent studies show that $\delta^{13}C$ varies significantly with time and space at Turrialba (Malowany et al., 2017). Hilton et al. (2010) suggested that temporal changes in $CO_2/^3He$ and $\delta^{13}C$ at Turrialba in low-temperature gas samples (i.e., boiling-point fumaroles) were due to varying contributions from mantle versus subduction fluids. However, Barry et al. (2013, 2014) show that these ratios can vary greatly by fractionation due to both magmatic degassing and phase separation in the hydrothermal system. Rizzo et al. (2016) argue that variations in $^3He/^4He$ at Turrialba are related to mixing between hydrothermal fluids and magmatic gas, not variations in mantle versus subduction fluid components as argued by Hilton et al. (2010). Given that extremely large variations in hydrothermal versus magmatic gas contribution are observed even in the high-flux vent gases at Turrialba (de Moor et al., 2016a), dismissing shallow hydrothermal (i.e., shallow crustal source) versus magmatic factors in favor of mantle versus subduction fluid (i.e., recycled sedimentary/crustal source) contributions seems suspect based on samples from low-temperature hydrothermal gas emissions. Furthermore, whereas high-temperature gases (i.e., much higher than boiling point) may not be affected by phase separation modification of $CO_2/^3He$ and $\delta^{13}C$, these ratios may still be subject to significant magmatic-degassing fractionation processes (Barry et al., 2014). More work is needed to understand these processes and to distinguish the relative contributions of mantle versus subducted carbon at subduction zones. Perhaps the most important implication from this study is that arc systems may show significant temporal variations in gas-emission rate, which can drastically change the mass balance at subduction zones from net "ingassing" to net "outgassing."

There are numerous sources of arc-related CO_2 degassing not considered in our value of 22,500 ± 4,940 T/d. Diffuse CO_2 degassing occurs at all volcanoes and may contribute significantly to the total C flux from the arc. Epiard et al. (2017) reported diffuse CO_2 degassing fluxes of 115 ± 46 T/d for Turrialba in 2013, 5.8 ± 0.5 T/d for Poás in 2012, and 15 ± 12 T/d for Irazú in 2015. These results suggest that about 10% of total CO_2 degassed is released as diffuse degassing at SCAVA volcanoes. Lucic et al. (2014) estimated that the diffuse CO_2 flux from Cerro Negro was 31 ± 5 T/d in 2012. Salazar et al. (2001) measured a diffuse CO_2 of 2,800 T/d at Cerro Negro after the 1999 eruption and Barrancos et al. (2013) showed that the flux since decreased steadily with time. Perez et al. (2000) measured ~1,700 T/d of diffuse CO_2

degassing at Masaya caldera in 1999. Thus, known diffuse degassing fluxes could easily contribute an additional 10% to the CO_2 output of the arc.

SCAVA also hosts various sizeable calderas including Guayabo and Cañas Dulces calderas in northern Costa Rica, and Cosigüina and Apoyo calderas in Nicaragua with unknown diffuse-degassing contributions. Both calderas in northern Costa Rica are greater than 15 km in diameter and host extensive active hydrothermal systems that are exploited for geothermal energy. Considering that both release CO_2-rich gases and that the combined energy output from the geothermal projects contributes ~15% of the total energy used in Costa Rica, it seems highly likely that these two systems contribute significantly to the total arc degassing budget. Similar sized calderas are known to produce large amounts of CO_2. For example, Campi Flegrei (10 km diameter) in Italy releases ~1,500 T/d (Chiodini et al., 2001). Combined, Costa Rica and Nicaragua produced 240 MW from geothermal power from volcanic hydrothermal systems in 2004 (Birkle & Bundschuh, 2007), and that value has subsequently approximately doubled. Considering the relationship between geothermal power and CO_2 flux expressed in Chiodini et al. (2005), this energy flux could represent more than 6,000 T/d CO_2, which seems reasonable considering the presence of large calderas such as Canas Dulces, Guayabo, Masaya, Consiguina, and Apoyo. The total geothermal energy reserve in Costa Rica and Nicaragua is far higher than the current geothermal production capacity and is estimated at 6,240 MW (Birkle & Bundschuh, 2007). Thus, the potential CO_2 flux contribution from geothermal systems is most likely significant, essentially unconstrained, and warrants further investigation. Fore-arc degassing along faults could be another significant contributor to the total output of the subduction zone, though we have no constraints on the flux.

Based on our data set and considerations of other unaccounted for degassing sources, it seems likely that the total arc CO_2 flux from SCAVA is currently higher than the total C input via subduction.

4.3.6. Tectonic Controls on Temporal Variations in Arc-Scale Gas Emission?

Comparison of our estimates of total gas fluxes from SCAVA with previous estimates perhaps suggests that degassing has been more intense in the last few years than since the instrumental record began in the mid-1980s (Table 4; see discussion in section 4.3.1). Figure 10 shows that SCAVA has also experienced more volcanic eruptions in the 2015–2016 period than in any period since 1980 based on the Smithsonian Global

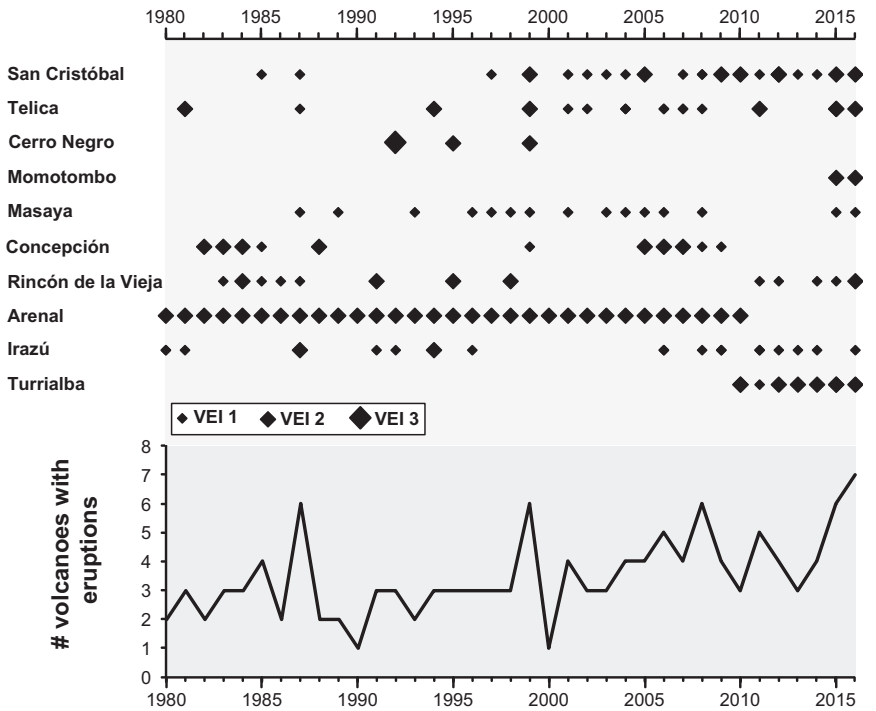

Figure 10. (top) Occurrence of eruptions at SCAVA volcanoes. Small diamonds = VEI 1, medium diamonds = VEI 2, large diamonds = VEI ≥ 3. Lower plot shows the number of volcanoes with eruptions per year. Data from Smithsonian Global Volcanism Program.

Volcanism Program (2013) database. One potential explanation for temporal variations in arc degassing could be that physical changes in the arc crust (e.g., changes in the stress field) on the regional scale play a role in the level of volcanic activity (e.g., La Femina, 2015) and intensity of degassing. Recently, Carn et al. (2017) showed that temporal variations in arc-scale degassing have been observed in decadal records of OMI satellite measurements.

Tectonic and magmatic systems are intimately connected within plate boundary zones. Earthquakes change the state of stress within the crust, allowing for the opening of pathways and migration of magmas and therefore gases. Several subduction zone megathrust and upperplate earthquakes have occurred along the SCAVA segment of the Central American Volcanic Arc during the 26 year period shown in Figure 10. We are interested here in earthquakes that predate the increase in activity shown by our gas flux data. Two large earthquakes occurred along the SCAVA in late 2012. The Mw 7.3 El Salvador earthquake struck on 27 August 2012 at 10:37 P.M. local time offshore of the El Salvador-Nicaragua border (Geirsson et al., 2015). This was followed by the Mw 7.6 Nicoya earthquake, which occurred at 8:42 am local time on 5 September 2012 directly beneath the Nicoya peninsula (Protti et al., 2014). The areas of slip on the megathrust fault are shown for each earthquake in Figure 1. Prior to the Nicoya earthquake the arc crust in northern Costa Rica was under compression, which was demonstrated by the OVSICORI GPS network (Protti et al., 2014). About 1.5 m of thrust occurred on the megathrust fault during the earthquake, displacing the fore-arc trenchward. This displacement resulted in a reversal of stress regime in the arc from compressional to extensional (Figure 11). Similar observations were made in Chile after the Maule earthquake in Central Chile (Farías et al., 2011).

The volcanic arc in Nicaragua is more complicated, as the arc-forearc system is dominated by northwest directed forearc translation at $\sim$11 mm $^{-a}$ (Kobayashi et al., 2014 and references therein). The Mw7.3 El Salvador earthquake caused co-seismic and post-seismic displacements at coastal geodetic sites; however, geodetic sites located in the Maribios Range (e.g., at San Cristobal, Telica, and Cerro Negro volcanoes) did not measure significant displacements.

A tantalizing interpretation of the higher gas fluxes and increased volcanic activity observed at SCAVA is that a shift to extensional stress regime resulted in relaxation of volcanic edifices and facilitated movement of magma and volatiles through opened conduits. Many volcanoes displayed increased activity in the years following the Nicoya and El Salvador earthquakes. San Cristobal erupted on 8 September 2012, sending ash to 5 km just 9 days after the El Salvador earthquake and 3 days after the Nicoya earthquake. Telica experienced its largest eruption in decades on 22 November 2015, producing a column up to 8 km. In December 2015 Momotombo erupted for the first time in over a century, producing a lava flow and frequent strombolian to vulcanian eruptions. A lava lake appeared at Masaya for the first time since the 1990s following the 2012 earthquakes and the Lake Managua earthquake sequence in 2014. Concepción experienced a seismic crisis in mid-2015 but has not erupted. Rincón de la Vieja has produced numerous phreatic eruptions in recent years with eruptive columns up to 2 km. Small phreatic eruptions have also been extremely common at Poás in recent years, and in 2017 produced a phreatomagmatic eruption for the first time since 1953. Activity at Turrialba volcano increased significantly in 2014, from isolated vent opening eruptions between 2010 and 2014 and very frequent ash emissions thereafter with occasional columns up to 4 km.

In comparison with previous studies, our data suggest that both the SO_2 and CO_2 gas fluxes have increased dramatically at SCAVA. The qualitative observation of increased volcanic activity lends support to the assertion that degassing has quantitatively increased at the arc (see section 4.3.1). Our Multi-GAS data set also suggest that the bulk arc CO_2/SO_2 ratio has increased relative to data presented in Aiuppa et al. (2014, 2017), suggesting deeper gas sources (e.g., de Moor et al., 2016a). A conceptual model that links the tectonic and volcanologic observations is presented in Figure 12. Trenchward displacement in the fore arc due to megathrust earthquakes results in a change from a compressional to extensional stress regime, opening arc-parallel conduits that allow the release of deeply stored volatiles and magma. Our data set suggests high gas fluxes from SCAVA and that these gases have a deeper source than in previous surveys. Temporal variation in arc output at the regional scale could ultimately be related to physical processes within the upper plate.

There are several caveats to this hypothesis. First, large uncertainties exist in decadal-scale time series of gas emissions at SCAVA, as discussed in detail in section 4.3.1. Second, the temporal coupling between

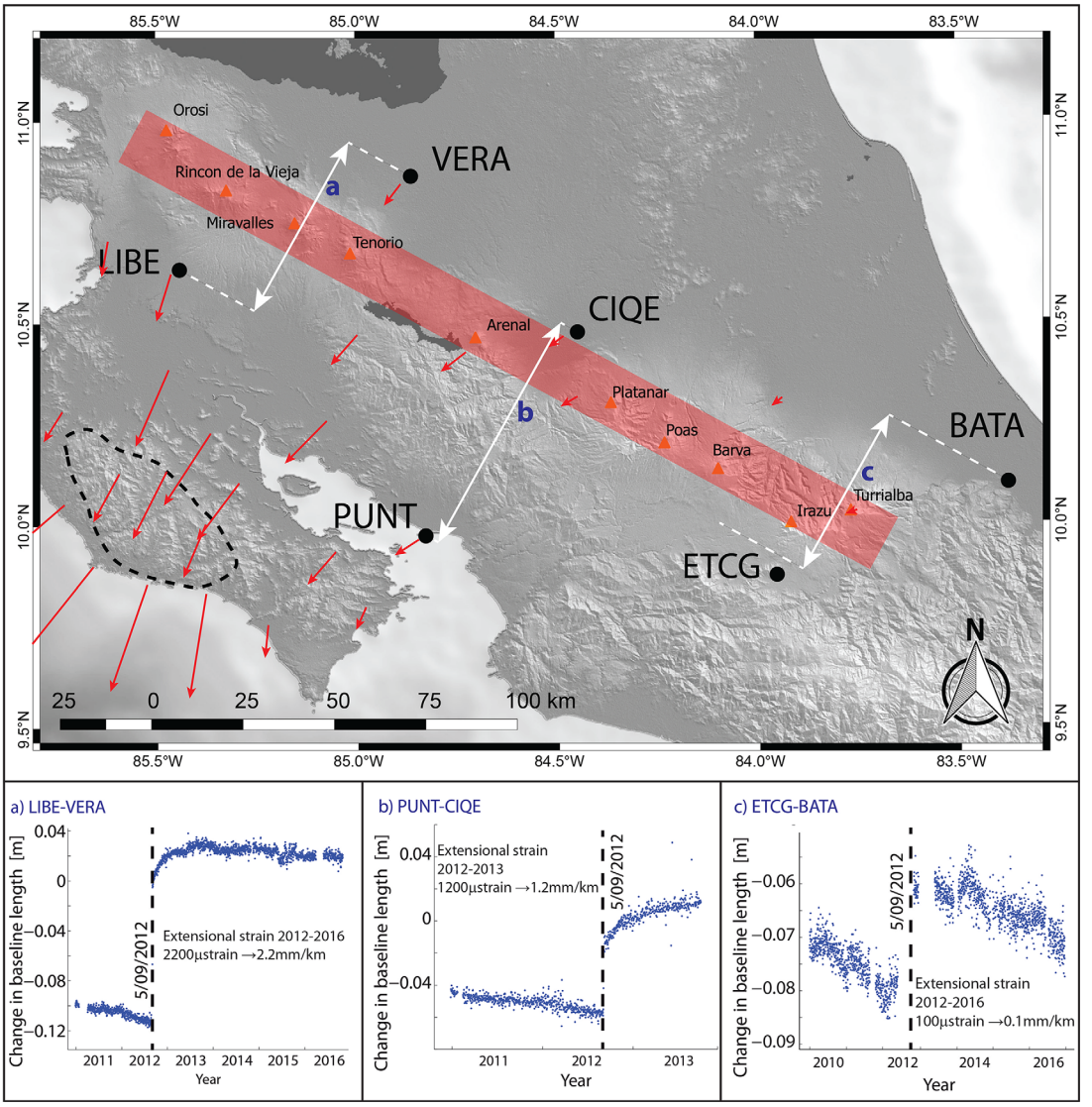

Figure 11. Extensional strain on the Costa Rican volcanic arc after the 5 September 2012 Nicoya earthquake. The dashed perimeter shows the rupture extent of the Mw 7.6 Earthquake. The red arrows show the coseismic movement at the GPS sites. The red rectangle shows the Costa Rican volcanic front and the orange triangles are the volcanic edifices. Subplots (a)–(c) show the variation of perpendicular-arc-distance over time between the selected GPS pairs (a) LIBE and VERA, (b) CIQE and PUNT, and (c) ETCG and BATA located on either side of the volcanic front.

earthquakes and volcanism is not well understood (e.g., LaFemina, 2015). Previous studies on the subject have mostly pointed to short times between local earthquakes and eruptions as the strongest evidence for a causative link. On the regional scale the delay between earthquakes and volcano activation may be greater. Third, two large meagathrust earthquaked occurred in 1990 (Mw 7.3) and 1992 (Mw 7.6) on the coast of Costa Rica and off the coast of Nicaragua, respectively (Ekström et al., 2012). Gas emission data for this period are insufficient to assess arc degassing changes in response to these earthquakes. Fourth, there are many exceptions to the hypothesis that SCAVA volcanoes became more active after the Nicoya and El Salvador earthquakes. Arenal volcano, for example, was highly active between 1968 and 2010. Gas flux has remained extremely low after 2012 and no eruptive activity has occurred, yet Arenal is the closest active volcano to the Nicoya earthquake epicenter. Irazú is one of the most active volcanoes in the arc (Figure 10), but also has not erupted or shown increased degassing. Likewise, Cerro Negro volcano has shown no clear increase in activity. Fourth, other volcanoes such as Poás and Turrialba displayed eruptive activity prior to 2012, and numerous studies have suggested that this unrest was due to magmatic intrusions that occurred around the turn of the millenium. This suggests that our data may show an apparent increase in gas flux

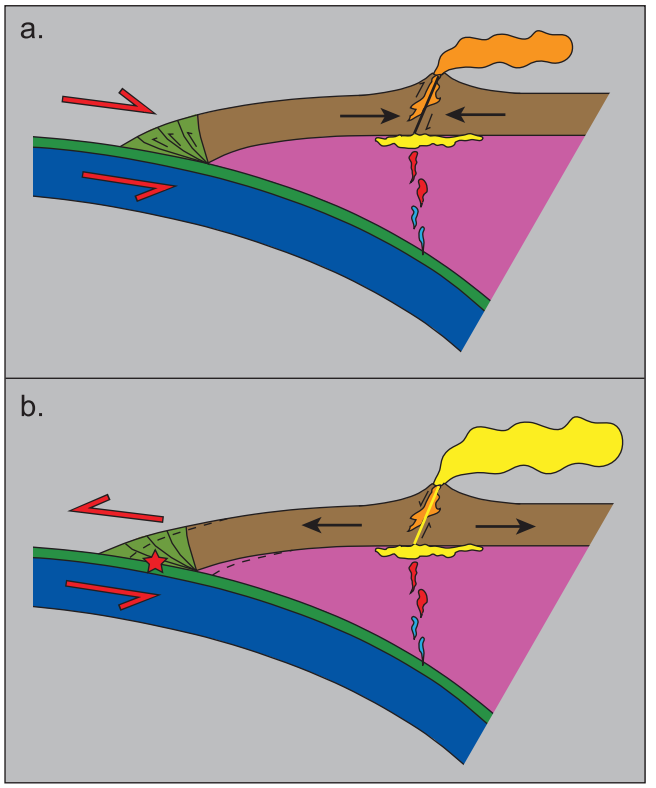

Figure 12. Cartoon showing a conceptual model linking crustal response to large earthquakes to increased volcanic degassing and activity. Prior to megathrust earthquakes (a) the forearc is locked to the downgoing slab and the upper plate hosting the active volcanic arc is under compression. Slip occurs on the megathrust (b) the forearc is displaced trenchward, and the volcanic arc experiences extension. Volcanic conduits between deep crustal magma reservoirs and the surface relax, allowing the release of deep magmatic gases.

with the earthquakes, but increase in arc degassing may in fact have begun beforehand. On the other hand, the data of Aiuppa et al. (2014) were collected in 2013 but do not suggest an increase in degassing compared to previous studies. However, some of the flux values in Aiuppa et al. (2014) may be significantly underestimated (see section 4.3.1). Thus, attempts to establish a link between the Nicoya and El Salvador earthquakes and increased degassing at the SCAVA arc remain speculative with the currently available data.

An important outcome of this study is that time series gas data has great potential to yield new insights into tectonic-scale processes if monitoring were conducted on similar scale to traditional geophysical methods. We are currently limited by noncontinuous measurements at only a few volcanoes in the global context. Large uncertainties in some gas flux methodologies also need to be improved in order to resolve more subtle changes in gas output at the majority of low gas emitting arc volcanoes. Whereas the global volatile output may be approximated by simultaneous measurement of gas fluxes at the larges emitters, many outstanding questions will remain. Here we have highlighted that within SCAVA, arc outputs are highly variable through time and space. In contrast to previous studies, we suggest that arc volatile budgets are strongly influenced by relatively short-lived degassing events (e.g., Turrialba, Miyakejima, Popocateptl) on geologic timescales and that entire arc systems may display dramatic short-term variations in volatile output.

5. Conclusions

In this contribution we have presented ~300 new SO_2 flux measurements at 10 actively degassing volcanoes of the Southern Central American Volcanic Arc: Turrialba, Poás, Arenal, Rincón de la Vieja, Concepción, Masaya, Momotombo, Cerro Negro, Telica, and San Cristobal volcanoes in Costa Rica and Nicaragua. The SO_2 flux data set is internally consistent as all measurements were achieved with vertically pointing DOAS spectrometers traversed beneath volcanic plumes, and plume speeds were derived from NOAA NCEP GFS models calibrated using direct anemometer measurements at a subset of volcano summits. We have also presented new Multi-GAS data collected contemporaneously at nine of these volcanoes as well as new data for three hydrothermal systems.

Our data set constrain the volatile flux at SCAVA from active degassing in 2015–2016 to 6,240 ± 1,150 T/d SO_2 and 22,540 ± 4,940 T/d CO_2. Neither SO_2 nor CO_2 flux distributions follow a power law. Our total fluxes are significantly higher than those previously reported for SCAVA, in part due to our more comprehensive survey of the arc but also due to increased volcanic degassing (and eruptive activity) on the arc. We challenge the commonly held assertion in volatile budget calculations that volcanic degassing is either passive and constant or eruptive and instantaneously high. On the contrary, baseline "passive" degassing is variable and related to general state of volcanic activity/dormancy and eruptive degassing varies from slightly above baseline during low energy eruptive activity to highly elevated during eruptive release of accumulated volatiles. These dynamic variations occur over orders of magnitude in terms of gas emission rate, and variations at the arc scale probably occur at sufficient magnitude as to significantly alter regional volatile budgets.

It is likely that the net CO_2 flux from SCAVA in 2015–2016 was higher than the total CO_2 input, however the uncertainties involved in input and output estimates preclude a robust conclusion. The net influx of CO_2 from subducted sediments, oceanic crust, serpentinized mantle, and subduction erosion is estimated at ~24,000 T/d—within error of the CO_2 outflux from volcanoes. Diffuse CO_2 degassing in the immediate vicinity of active volcanic craters likely adds >10% to the total arc flux. Large caldera-hosted hydrothermal systems in Costa Rica and Nicaragua likely add > 5,000 T/d CO_2, though this is unconstrained. The CO_2 flux

from diffuse degassing along faults in the forearc and back arc are completely unknown but may be significant. Quantification of these unknown fluxes are a prime target for future research at SCAVA, as at arc systems globally. Our data suggest that C input to the deep mantle via Central American subduction, previously thought to be more efficient than at other arcs, has been overestimated.

The C/S ratio in volcanic gases is variable at any given volcano and has been shown by previous studies to correlate with volcanic activity. Our estimate for the bulk C/S ratio of SCAVA is ∼5.1, which is higher than prior estimates. The C/S ratio of bulk arc output in Costa Rica is slightly lower than that in Nicaragua, at 4.8 versus 5.4, respectively. The bulk C/S ratio of subduction input in the Costa Rican (∼6.1) segment of the arc is also lower than in the Nicaraguan segment (∼7.1) due to more relative contribution from igneous crust and subduction erosion in Costa Rica, both of which contribute to low C/S. Higher CO_2/SO_2 ratio in our data set is observed relative to previous studies, further suggesting temporal variation in arc-scale degassing.

We propose that temporal variations in arc-scale degassing may be related to stress changes in the overriding plate following large seismic events. Time-series data sets of volcanic degassing may indeed be the best way to quantify increases in volcanic output on regional scales. However, robust and internally consistent degassing data sets need to be improved in both spatial and temporal coverage as well as in accuracy and uncertainty before causative relationships between arc-scale volcanic activity and tectonic-scale seismic events can be established. High-frequency gas monitoring has identified immediate precursors to volcanic eruptions and is also essential to accurately constraining global volatile budgets. Nascent gas monitoring networks should be expanded to similar scales as traditional geophysical networks in order to link tectonic processes with arc degassing and volcanic activity.

Acknowledgments
We would like to thank one anonymous reviewer and the editor, Cin-ty Lee, for constructive comments that improved this article. Jake Lowenstern is kindly thanked for a helpful review of a previous version of the manuscript. OVSICORI personnel are grateful to the Ley Transitorio 8933 for funding associated with volcano monitoring. JMdM appreciatively acknowledges support from the Deep Carbon Observatory Reservoirs and Fluxes Program, as well as support for the "Biology Meets Subduction" early-career scientist project in Costa Rica. Additional instruments and support were provided by USGS-VDAP program and JMdM would also like to thank Peter Kelly for providing a Multi-GAS instrument that continues monitoring gas emissions at Turrialba volcano. The data presented in this work can be found in the supporting information file.

References

Ague, J. J., & Nicolescu, S. (2014). Carbon dioxide released from subduction zones by fluid-mediated reactions. *Nature Geoscience*, *7*, 355–360.

Aiuppa, A., Federico, C., Giudice, G., Giuffrida, G., Guida, R., Gurrieri, S., . . . Papale, P. (2009). The 2007 eruption of Stromboli volcano: Insights from the real-time measurement of the volcanic gas plume CO_2/SO_2 ratio. *Journal of Volcanology and Geothermal Research*, *182*, 221–230.

Aiuppa, A., Fischer, T., Plank, P., Robidoux, T. P., & Napoli, R. D. (2017). Along-arc, inter-arc and arc-to-arc variations in volcanic gas CO 2/S T ratios reveal dual source of carbon in arc volcanism. *Earth-Science Reviews*, *168*, 24–47.

Aiuppa, A., Inguaggiato, S., McGonigle, A. J. S., O'dwyer, M., Oppenheimer, C., Padgett, M. J., . . . Valenza, M. (2005). H2S fluxes from Mt. Etna, Stromboli, and Vulcano (Italy) and implications for the sulfur budget at volcanoes. *Geochimica et Cosmochimica Acta*, *69*, 1861–1871.

Aiuppa, A., Moretti, R., Federico, C., Giudice, G., Gurrieri, S., Liuzzo, M., . . . Valenza, M. (2007). Forecasting Etna eruptions by real-time observation of volcanic gas composition. *Geology*, *35*, 1115–1118.

Aiuppa, A., Robidoux, P., Tamburello, G., Conde, V., Galle, B., Avard, G., . . . Muñóz, A. (2014). Gas measurements from the Costa Rica-Nicaragua volcanic segment suggest possible along-arc variations in volcanic gas chemistry. *Earth and Planetary Science Letters*, *407*, 134–147.

Allard, P. (1983). The origin of hydrogen, carbon, sulphur, nitrogen and rare gases in volcanic exhalations: Evidence from isotope geochemistry. In edited by H. A. Sabroux & J. C. Tazieff (Eds.), *Forecasting volcanic events* (pp. 337–386). Amsterdam, the Netherlands: Elsevier.

Allard, P. (1992). Global emissions of helium-3 by subaerial volcanism. *Geophysical Research Letters*, *19*, 1479–1481.

Alt, J. C., Garrido, C. J., Shanks, W. C., Turchyn, A., Padron-Navarta, J. A., Sanchez-Vizcaino, V. L., . . . Marchesi, C. (2012). Recycling of water, carbon, and sulfur during subduction of serpentinites: A stable isotope study of Cerro del Almirez, Spain. *Earth and Planetary Science Letters*, *327*, 50–60.

Alt, J. C., Schwarzenbach, E. M., Früh-Green, G. L., Shanks, W. C., Bernasconi, S. M., Garrido, C. J., . . . Marchesi, C. (2013). The role of serpentinites in cycling of carbon and sulfur: Seafloor serpentinization and subduction metamorphism. *Lithos*, *178*, 40–54.

Alt, J. C., Shanks, W. C., Bach, W., Paulick, H., Garrido, C. J., & Beaudoin, G. (2007). Hydrothermal alteration and microbial sulfate reduction in peridotite and gabbro exposed by detachment faulting at the Mid-Atlantic Ridge, 15 degrees 20 ′ N (ODP Leg 209): A sulfur and oxygen isotope study. *Geochemistry Geophysics Geosystems*, *8*, Q08002. https://doi.org/10.1029/2007GC001617

Alvarado, G. E., Mele, D., Dellino, P., de Moor, J. M., & Avard, G. (2016). Are the ashes from the latest eruptions (2010–2016) at Turrialba volcano (Costa Rica) related to phreatic or phreatomagmatic events? *Journal of Volcanology and Geothermal Research*, *327*, 407–415.

Andres, R. J., & Kasgnoc, A. D. (1998). A time-averaged inventory of subaerial volcanic sulfur emissions. *Journal of Geophysical Research*, *103*, 25251–25261.

Barrancos, J., Ibarra, M., Melián, G., Álvarez, J., Rodriguez, F., Nolasco, D., . . . Munoz, A. (2013). Diffuse CO2 monitoring at Cerro Negro volcano, Nicaragua. In *International Association of Volcanology and Chemistry of the Earth's Interior (IAVCEI) Scientific Assembly, Kagohsima (Abstract 3W_2G-P11)*, Kagoshima, Japan.

Barry, P. H., Hilton, D. R., Fischer, T. P., de Moor, J. M., Mangasini, F., & Ramirez, C. (2013). Helium and carbon isotope systematics of cold "mazuku" CO_2 vents and hydrothermal gases and fluids from Rungwe Volcanic Province, southern Tanzania. *Chemical Geology*, *339*, 141–156.

Barry, P. H., Hilton, D. R., Füri, E., Halldorsson, S. A., & Grönvold, K. (2014). Carbon isotope and abundance systematics of Icelandic geothermal gases, fluids and subglacial basalts with implications for mantle plume-related CO2 fluxes. *Geochimica et Cosmochimica Acta*, *134*, 74–99.

Beirle, S., Sihler, H., & Wagner, T. (2013). Linearisation of the effects of spectral shift and stretch in DOAS analysis. *Atmospheric Measurement Techniques*, *6*, 661–675. https://doi.org/610.5194/amt-5196-5661-2013

Bertani, R. (2012). Geothermal power generation in the world 2005–2010 update report. *Geothermics*, *41*, 1–29.
Birkle, P., & Bundschuh, J. (2007). High and low enthalpy geothermal resources and potentials. In J. Bundschuh & G. E. Alvarado (Eds.), *Central America: Geology, resources and hazards* (pp. 707–777). Leiden, the Netherlands: Taylor & Francis.
Bogumil, K., Orphal, J., Homann, T., Voigt, S., Spietz, P., Fleischmann, O. C., . . . Burrows, J. P. (2003). Measurements of molecular absorption spectra with the SCIAMACHY pre-flight model: Instrument characterization and reference data for atmospheric remote-sensing in the 230–2380 nm region. *Journal of Photochemistry Photobiology A: Chemistry*, *157*, 167–184.
Boucher, C., Bernard, M., Lan, T., Fischer, T. P., Dereje, A., Mabrya, J., . . . Zimmermann, L. (2017), Atmospheric helium isotope composition as a tracer of volcanic emissions: A case study of Erta Ale volcano, Ethiopia, *Chemical Geology*. https://doi.org/10.1016/j.chemgeo.2017.05.011, http://www.sciencedirect.com/science/article/pii/S000925411730298X, in press.
Brantley, S. L., & Koepenick, K. W. (1995). Measured carbon-dioxide emissions from Oldoinyo-Lengai and the skewed distribution of passive volcanic fluxes. *Geology*, *23*, 933–936.
Burdett, J. W., Arthur, M. A., & Richardson, M. (1989). A neogene seawater sulfur isotope age curve from calcareous pelagic microfossils. *Earth and Planetary Science Letters*, *94*, 189–198.
Burton, M. R., Sawyer, G. M., & Granieri, D. (2013). Deep carbon emissions from volcanoes. In R. M. Hazen et al. (Eds.), *Carbon in earth* (pp. 323–354). Chantilly, VA: Mineralogical Society of America.
Campion, R., Delgado-Granados, H., & Mori, T. (2015). Image-based correction of the light dilution effect for SO 2 camera measurements. *Journal of Volcanology and Geothermal Research*, *300*, 48–57.
Campion, R., Martinez-Cruz, M., Lecocq, T., Caudron, C., Pacheco, J., Pinardi, G., . . . Bernard, A. (2012). Space- and ground-based measurements of sulphur dioxide emissions from Turrialba Volcano (Costa Rica). *Bulletin of Volcanology*, *74*, 1757–1770.
Carn, S. A., Fioletov, V. F., McLinden, C. A., Li, C., & Krotkov, A. (2017). A decade of global volcanic SO2 emissions measured from space. *Scientific Reports*, *7*, 44095. https://doi.org/10.1038/srep44095
Carn, S. A., Krotkov, N. A., Yang, K., & Krueger, A. J. (2013). Measuring global volcanic degassing with the Ozone Monitoring Instrument (OMI). *Geological Society Special Publications*, *380*, 229–257.
Chiodini, G., Cardellini, C., Amato, A., Boschi, E., Caliro, S., Frondini, F., & Ventura, G. (2003). Carbon dioxide Earth degassing and seismogenesis in central and southern Italy. *Geophysical Research Letters*, *31*, L07615. https://doi.org/07610.01029/02004GL019480
Chiodini, G., Frondini, F., Cardellini, C., Granieri, D., Marini, L., & Ventura, G. (2001). CO_2 degassing and energy release at Solfatara volcano, Campi Flegrei, Italy. *Journal of Geophysical Research*, *106*, 16213–16221.
Chiodini, G., Granieri, D., Avino, R., Caliro, S., Costa, A., & Werner, C. (2005). Carbon dioxide diffuse degassing and estimation of heat release from volcanic and hydrothermal systems. *Journal of Geophysical Research*, *110*, B08204. https://doi.org/10.1029/2004JB003542
Christopher, T. E., Blundy, J., Cashman, K., Cole, P., Edmonds, M., Smith, P. J., . . . Stinton, A. (2015). Crustal-scale degassing due to magma system destabilization and decoupling at Soufrière Hills Volcano, Monteserrat. *Geochemistry, Geophysics, Geosystems*, *16*, 2797–2811, https://doi.org/10.1002/2015GC005791
Conde, V., Bredemeyer, S., Duarte, E., Pacheco, J., Miranda, S., Galle, B., & Hansteen, T. H. (2013). SO_2 degassing from Turrialba Volcano linked to seismic signatures during the period 2008–2012. *International Journal of Earth Science*, *103*(7), 1983–1998. https://doi.org/10.1007/s00531-00013-00958-00535
D'Aleo, R., Bitetto, M., Delle Donne, D., Tamburello, G., Battaglia, A., Coltelli, M., . . . Aiuppa, A. (2016). Spatially resolved SO2 flux emissions from Mt Etna. *Geophysical Research Letters*, *43*, 7511–7519. https://doi.org/10.1002/2016GL069938
Dasgupta, R. (2013). Ingassing, storage, and outgassing of terrestrial carbon through geologic time. *Reviews in Mineralogy and Geochemistry*, *75*, 183–229.
de Moor, J. M., Aiuppa, A., Avard, G., Wehrmann, H., Dunbar, N., Muller, C., . . . Conde, V. (2016a). Turmoil at Turrialba Volcano (Costa Rica): Degassing and eruptive processes inferred from high-frequency gas monitoring. *Journal of Geophysical Research: Solid Earth*, *121*, 5761–5775. https://doi.org/10.1002/2016JB013150
de Moor, J. M., Aiuppa, A., Pacheco, J., Avard, G., Kern, C., Liuzzo, M.,, . . . Fischer, T. P. (2016b). Short-period volcanic gas precursors to phreatic eruptions: Insights from Poás Volcano, Costa Rica. *Earth and Planetary Science Letters*, *442*, 218–227. https://doi.org/10.1016/j.epsl.2016.1002.1056
de Moor, J. M., Fischer, T. P., Hilton, D. R., Hauri, E., Jaffe, L. A., & Camacho, J. T. (2005). Degassing at Anatahan volcano during the May 2003 eruption: Implications from petrology, ash leachates, and SO_2 emissions. *Journal of Volcanology and Geothermal Research*, *146*, 117–138.
de Moor, J. M., Fischer, T. P., Sharp, Z. D., King, P. L., Wilke, M., Botcharnikov, R. E., . . . Ramirez, C. (2013). Sulfur degassing at Erta Ale (Ethiopia) and Masaya (Nicaragua): Implications for degassing processes and oxygen fugacities of basaltic systems. *Geochemistry, Geophysics, Geosystems*, *14*, 4076–4108. https://doi.org/10.1002/ggge.20255
Duncan, M. S., & Dasgupta, R. (2017). Rise of Earth's atmospheric oxygen controlled by efficient subduction of organic carbon. *Nature Geoscience*, *10*, 387–392. https://doi.org/10.1038/ngeo2939
Ekström, G., Nettles, M., & Dziewonski, A. M. (2012). The global CMT project 2004–2010: Centroid-moment tensors for 13,017 earthquakes. *Physics of the Earth and Planetary Interiors*, *200–201*, 1–9. https://doi.org/10.1016/j.pepi.2012.1004.1002
Elkins, L. J., Fischer, T. P., Hilton, D. R., Sharp, Z. D., McKnight, S., & Walker, J. (2006). Tracing nitrogen in volcanic and geothermal volatiles from the Nicaraguan volcanic front. *Geochimica et Cosmochimica Acta*, *70*, 5215–5235.
Epiard, M., Avard, G., de Moor, J. M., Martínez Cruz, M., Barrantes Castillo, G., & Bakkar, H. (2017). Relationship between diffuse CO2 degassing and volcanic activity. Case study of the Poás, Irazú, and Turrialba Volcanoes, Costa Rica. *Frontiers in Earth Science*, *5*, 71.
Evans, K. A. (2012). The redox budget of subduction zones. *Earth-Science Reviews*, *113*, 11–32.
Farías, M., Comte, D., Roecker, S., Carrizo, D., & Pardo, M. (2011). Crustal extensional faulting triggered by the 2010 Chilean earthquake: The Pichilemu Seismic Sequence. *Tectonics*, *30*, TC6010. https://doi.org/10.1029/2011TC002888
Fischer, T. P. (2008). Fluxes of volatiles (H_2O, CO_2, N_2, Cl, F) from arc volcanoes. *Geochemical Journal*, *42*, 21–38.
Fischer, T. P., Hilton, D. R., Zimmer, M. M., Shaw, A. M., Sharp, Z. D., & Walker, J. A. (2002). Subduction and recycling of nitrogen along the central American margin. *Science*, *297*, 1154–1157.
Fischer, T. P., Ramirez, C., Mora-Amador, R. A., Hilton, D. R., Barnes, J. D., Sharp, Z. D., . . . Shaw, A. M. (2015). Temporal variations in fumarole gas chemistry at Poás volcano, Costa Rica. *Journal of Volcanology and Geothermal Research*, *294*, 56–70.
Freundt, A., Grevemeyer, I., Rabbel, W., Hansteen, T. H., Hensen, C., Wehrmann, H., . . . Frische, M. (2014). Volatile (H_2O, CO_2, Cl, S) budget of the Central American subduction zone. *International Journal of Earth Sciences*, *103*, 2101–2127. https://doi.org/10.1007/s00531-00014-01001-00531
Galle, B., Johansson, M., Rivera, C., Zhang, Y., Kihlman, M., Kern, C., . . . Hidalgo, S. (2010). Network for Observation of Volcanic and Atmospheric Change (NOVAC): A global network for volcanic gas monitoring: Network layout and instrument description. *Journal of Geophysical Research*, *115*, D05304. https://doi.org/10.1029/2009JD011823

Galle, B., Oppenheimer, C., Geyer, A., McGonigle, A. J. S., Edmonds, M., & Horrocks, L. (2002). A miniaturized ultraviolet spectrometer for remote sensing of SO2 fluxes: A new tool for volcano surveillance. *Journal of Volcanology and Geothermal Research*, *119*, 241–254.

Geirsson, H., LaFemina, P. C., DeMets, C., Hernandez, D. A., Mattioli, G. S., Rogers, R., . . . Tenorio, V. (2015). The 2012 August 27 Mw7. 3 El Salvador earthquake: Expression of weak coupling on the Middle America subduction zone. *Geophysical Journal International*, *202*, 1677–1689.

Giggenbach, W. F. (1987). Redox processes governing the chemistry of fumarolic gas discharges from White Island, New Zealand. *Applied Geochemistry*, *2*, 143–161.

Giggenbach, W. F. (1996). Chemical composition of volcanic gas. In R. Tilling (Ed.), *IAVCEI-UNESCO: Monitoring and mitigation of volcanic hazards* (pp. 221–256). Berlin, Germany: Springer-Verlag.

Global Volcanism Program (2013). Momotombo volcano. In E. Venzke (Ed.), *Volcanoes of the world v. 4.5.6*. Washington, DC: Smithsonian Institution. https://doi.org/10.5479/si.GVP.VOTW5474-2013

Grainger, J. F., & Ring, J. (1962). Anomalous Fraunhofer line profiles. *Nature*, *193*, 762.

Hilton, D. R., Fischer, T. P., & Marty, B. (2002). Noble gases and volatile recycling at subduction zones. In D. Porcelli, C. J. Ballentine, & R. Wieler (Eds.), *Noble gases in geochemistry and cosmochemistry* (pp. 319–370). Washington, DC: Mineralogical Society of America.

Hilton, D. R., Fischer, T. P., McGonigle, A. J. S., & de Moor, J. M. (2007). Variable SO_2 emission rates for Anatahan volcano, the Commonwealth of the Northern Mariana Islands: Implications for deriving arc-wide volatile fluxes from erupting volcanoes. *Geophysical Research Letters*, *34*, L14315. https://doi.org/10.1029/2007GL030405

Hilton, D. R., Ramirez, C., Mora-Amador, R., Fischer, T. P., Furi, E., Barry, P. H., & M. Shaw, A. (2010). Monitoring of temporal and spatial variations in fumarole helium and carbon dioxide characteristics at Poas and Turrialba volcanoes, Costa Rica (2001–2009). *Geochemical Journal*, *44*, 431–440.

Kelemen, P. B., & Manning, C. E. (2015). Reevaluating carbon fluxes in subduction zones, what goes down, mostly comes up. *Proceedings of the National Academy of Sciences of the United States of America*, *112*, E3997–E4006.

Kern, C., Deutschmann, T., Vogel, L., Wöhrbach, M., Wagner, T., & Platt, U. (2010). Radiative transfer corrections for accurate spectroscopic measurements of volcanic gas emissions. *Bulletin of Volcanology*, *72*, 233–247. https://doi.org/10.1007/s00445-00009-00313-00447

Kern, C., Sutton, J., Elias, T., Lee, L., Kamibayashi, K., Antolik, L., & Werner, C. (2015). An automated SO 2 camera system for continuous, real-time monitoring of gas emissions from Kīlauea Volcano's summit Overlook Crater. *Journal of Volcanology and Geothermal Research*, *300*, 81–94.

Kobayashi, D., LaFemina, P., Geirsson, H., Chichaco, E., Abrego, A. A., Mora, H., & Camacho, E. (2014). Kinematics of the western Caribbean: Collision of the Cocos Ridge and upper plate deformation. *Geochemistry, Geophysics, Geosystems*, *15*, 1671–1683. https://doi.org/10.1002/2014GC005234

La Femina, P. C. (2015). Plate tectonics and volcanism. In H. Sigurddson et al. (Eds.), *The encyclopedia of volcanoes* (2nd ed. pp. 65–92). London: Academic Press.

Lucic, G., Stix, J., Sherwood Lollar, B., Lacrampe-Couloume, G., Muñoz, A., & Carcache, M. I. (2014). The degassing character of a young volcanic center: Cerro Negro. *Nicaragua, Bulletin of Volcanology*, *76*(9), 850. https://doi.org/10.1007/s00445-00014-00850-00446

Malowany, K. S., Stix, J., de Moor, J. M., Chu, K., Lacrampe-Couloume, G., & Sherwood Lollar, B. (2017). Carbon isotope systematics of Turrialba volcano, Costa Rica, using a portable cavity ringdown spectrometer. *Geochemistry, Geophysics, Geosystems*, *18*, 2769–2784. https://doi.org/10.1002/2017GC006856

Marty, B., Jambon, A., & Sano, Y. (1989). Helium isotopes and CO2 in volcanic gases of Japan. *Chemical Geology*, *76*, 25–40.

Marty, B., & LeCloarec, M. F. (1992). Helium-3 and CO2 fluxes from subaerial volcanoes estimated from Polonium-210 emissions. *Journal of Volcanology and Geothermal Research*, *53*, 67–72.

Mason, E., Edmonds, M., & Turchyn, A. V. T. (2017). Heavy crustal carbon remobilized by arc volcanoes and implications for Earth's past. *Science*, *357*(6348), 290–294. https://doi.org/10.1126/science.aan5049

Mather, T. A., Pyle, D. M., Tsanev, V. I., McGonigle, A. J. S., Oppenheimer, C., & Allen, A. G. (2006). A reassessment of current volcanic emissions from the Central American arc with specific examples from Nicaragua. *Journal of Volcanology and Geothermal Research*, *149*, 297–311.

Menyailov, I. A., Nikitina, L. P., Shapar, V. N., & Pilipenko, V. P. (1986). Temperature increase and chemical change of fumarolic gases at Momotombo volcano, Nicaragua, in 1982–1985: Are these indicators of a possible eruption? *Journal of Geophysical Research*, *91*, 12199–12214.

Mori, T., Shinohara, H., Kazahaya, K., Hirabayashi, J., Matsushima, T., Mori, T., . . . Miyashita, M. (2013). Tim-averaged SO2 fluxes of subduction zone volcanoes: Example of a 32-year exhaustive survey for Japanese volcanoes. *Journal of Geophysical Research: Atmospheres*, *118*, 8662–8674. https://doi.org/10.1002/jgrd.50591

Oppenheimer, C. (1996). On the role of hydrothermal systems in the transfer of volcanic sulfur to the atmosphere. *Geophysical Research Letters*, *23*, 2057–2060.

Pérez, N., Salazar, J., Saballos, A., Álvarez, J., Segura, F., Hernández, P., & Notsu, K. (2000), Diffuse degassing of CO2 from Masaya caldera, Central America, Eos, Transactions American Geophysical Union, 81(48), Fall Meeting Supplement Abstract F1318.

Perez, N. M., Hernandez, P. A., Padilla, G., Nolasco, D., Barrancos, J., Melian, G., . . . Ibarra, M. (2011). Global CO_2 emission from volcanic lakes. *Geology*, *39*, 235–238.

Platt, U., & Stutz, J. (2008). *Differential Optical Absorption Spectroscopy: Principles and Applications* (597 pp.). Heidelberg, Germany: Springer.

Protti, M., González, V., Newman, A. V., Dixon, T. H., Schwartz, S. Y., Marshall, J. S., . . . Owen, S. E. (2014). Nicoya earthquake rupture anticipated by geodetic measurement of the locked plate interface. *Nature Geoscience*, *7*, 117–121.

Quisefit, J. P., Toutain, J. P., Bergametti, G., Javoy, M., Cheynet, B., & Person, A. (1989). Evolution versus cooling of gaseous volcanic emissions from Momotombo Volcano, Nicaragua: Thermochemical model and observations. *Geochimica et Cosmochimica Acta*, *53*, 2591–2608.

Ranero, C. R., Morgan, J. P., McIntosh, K., & Reichert, C. (2003). Bending-related faulting and mantle serpentinization at the Middle America trench. *Nature*, *425*, 367–373.

Ranero, C. R., & Weinrebe, W. (2005). Tectonic processes during convergence of lithospheric plates at subduction zones. In P. C. Wille (Ed.), *Sound images of the ocean* (pp. 85–105). Berlin, Germany: Springer.

Rizzo, A. L., Di Piazza, A., de Moor, J. M., Alvarado, G., Avard, E. G., Carapezza, M. L., & Mora, M. (2016). Eruptive activity at Turrialba volcano (Costa Rica): Inferences from 3He/4He in fumaroles gases and chemistry of ejected products, *Geochemistry, Geophysics, Geosystems*, *17*, 4478–4494. htpps://doi.org/10.1002/2016GC006525

Ruprecht, P., & Plank, T. (2013). Feeding andesitic eruptions with a high-speed connection from the mantle. *Nature*, *500*, 68–72.

Salazar, J. M., Hernández, P. A., Pérez, N. M., Melián, G., Álvarez, J., Segura, F., & Notsu, K. (2001). Diffuse emission of carbon dioxide from Cerro Negro volcano, Nicaragua, Central America. *Geophysical Research Letters*, *28*, 4275–4278.

Scambelluri, M., Bebout, G. E., Belmonte, D., Gilio, M., Campomenosi, N., Collins, N., & Crispini, L. (2016). Carbonation of subduction-zone serpentinite (high-pressure ophicarbonate; Ligurian Western Alps) and implications for the deep carbon cycling. *Earth and Planetary Science Letters*, *441*, 155–166.

Shaw, A. M., Hilton, D. R., Fischer, T. P., Walker, J. A., & Alvarado, G. E. (2003). Contrasting He-C relationships in Nicaragua and Costa Rica: Insights into C cycling through subduction zones. *Earth and Planetary Science Letters*, *214*, 499–513.

Shinohara, H. (2013). Composition of volcanic gases emitted during repeating Vulcanian eruption stage of Shinmoedake, Kirishima volcano, Japan. *Earth, Planets and Space*, *65*, 667–675. https://doi.org/610.5047/eps.2012.5011.5001

Stoiber, R. E., Malinconico, L. L., & Williams, S. N. (1983). Use of the correlation spectrometer at volcanoes. In H. S. Tazieff & J.-C. Sabroux (Eds.), *Forecasting volcanic events* (pp. 424–444). New York, NY: Elsevier.

Stoiber, R. E., Williams, S. N., & Huebert, B. J. (1986). Sulfur and halogen gases at Masaya Caldera complex, Nicaragua: Total flux and variations with time. *Journal of Geophysical Research*, *91*, 2215–2231.

Symonds, R. B., Gerlach, T. M., & Reed, M. H. (2001). Magmatic gas scrubbing: Implications for volcano monitoring. *Journal of Volcanology and Geothermal Research*, *108*, 303–341.

Symonds, R. B., Rose, W. I., Bluth, G. J. S., & Gerlach, T. M. (1994). Volcanic gas studies: Methods, results, and applications. In M. R. Caroll & J. R. Holloway (Eds.), *Reviews in mineralogy and geochemistry* (Vol. 30, pp. 1–66). Chantilly, VA: Mineralogical Society of America.

Tamburello, G., Agusto, M., Caselli, A., Tassi, F., Vaselli, O., Calabrese, S., . . . Aiuppa, A. (2015). Intense magmatic degassing through the lake of Copahue volcano, 2013–2014. *Journal of Geophysical Research Solid Earth*, *120*, 6071–6084. https://doi.org/10.1002/2015JB012160

Taran, Y., & Zelenski, M. (2014). Systematics of water isotopic composition and chlorine content in arc-volcanic gases. In G. F. Zellmer et al. (Eds.), *The role of volatiles in the genesis, evolution and eruption of arc magmas* (pp. 237–262). London: The Geological Society. https://doi.org/10.1144/SP1410.1145

Thomson, A. R., Walter, M. J., Kohn, S. C., & Brooker, R. A. (2016). Slab melting as a barrier to deep carbon subduction. *Nature*, *529*, 76–79.

Torgersen, T. (1989). Terrestrial helium degassing fluxes and the atmospheric helium budget: Implications with respect to the degassing processes of continental crust. *Chemical Geology*, *79*, 1–14.

Troll, V. R., Hilton, D. R., Jolis, E. M., Chadwick, J. P., Blythe, L. S., Deegan, F. M., . . . Zimmer, M. M. (2012). Crustal CO_2 liberation during the 2006 eruption and earthquake events at Merapi volcano, Indonesia. *Geophysical Research Letters*, *39*, L11302, https://doi.org/10.1029/2012GL051307

Tumiati, S., Tiraboschi, C., Sverjensky, D. A., Pettke, T., Recchia, S., Ulmer, P., . . . Poli, S. (2017). Silicate dissolution boosts the CO_2 concentrations in subduction fluids. *Nature Communications*, *8*, 616. https://doi.org/10.1038/s41467-41017-00562-z

Vandaele, A. C., Hermans, C., & Fally, S. (2009). Fourier transform measurements of SO2 absorption cross sections: II. Temperature dependence in the 29 000–44 000 cm-1 (227–345 nm) region. *Journal of Quantitative Spectroscopy and Radiative Transfer*, *110*, 2115–2126. https://doi.org/110.1016/j.jqsrt.2009.2105.2006

Vannucchi, P., Galeotti, S., Clift, P. D., Ranero, C. R., & von Huene, R. (2004). Long-term subduction-erosion along the Guatemalan margin of the Middle America Trench. *Geology*, *32*, 617–620.

Vannucchi, P., Ranero, C. R., Galeotti, S., Straub, S. M., Scholl, D. W., & McDougall-Ried, K. (2003). Fast rates of subduction erosion along the Costa Rica Pacific margin: Implications for non-steady rates of crustal recycling at subduction zones. *Journal of Geophysical Research*, *108*(B11), 2511. https://doi.org/10.1029/2002/B002207

Williams-Jones, G., Horton, K. A., Elias, T., Garbeil, H., Mouginis-Mark, P. J., Sutton, A. J., & Harris, A. J. (2006).Accurately measuring volcanic plume velocity with multiple UV spectrometers. *Bulletin of Volcanology*, *68*, 328–332.

Williams-Jones, G., Stix, J., Heiligmann, M., Barquero, J., Fernandez, E., & Gonzalez, E. D. (2001). A model of degassing and seismicity at Arenal Volcano, Costa Rica. *Journal of Volcanology and Geothermal Research*, *108*, 121–139.

Zimmer, M. M., Fischer, T. P., Hilton, D. R., Alvarado, G. E., Sharp, Z. D., & Walker, J. A. (2004). Nitrogen systematics and gas fluxes of subduction zones: Insights from Costa Rica arc volatiles. *Geochemistry, Geophysics, Geosystems*, *5*, Q05J11. https://doi.org/10.1029/2003GC000651

Erratum

In the originally published version of this article, there was a minor error in Figure 12: two horizontal arrows, in both panels of the figure, appeared as lines without arrowheads. The arrowheads indicate a change in stress regime. The figure has since been corrected, and this version may be considered the authoritative version of record.